Available online at www.sciencedirect.com

ScienceDirect

Geochimica et Cosmochimica Acta 145 (2014) 116–138

Geochimica et Cosmochimica Acta

www.elsevier.com/locate/gca

Vegetation impact on stream chemical fluxes: Mule Hole watershed (South India)

J. Riotte [a,b,*], J.C. Maréchal [b], S. Audry [a], C. Kumar [b], J.P. Bedimo Bedimo [c], L. Ruiz [a,d], M. Sekhar [b], M. Cisel [b], R. Chitra Tarak [b], M.R.R. Varma [b], C. Lagane [a], P. Reddy [b], J.J. Braun [a,b]

[a] *Géosciences Environnement Toulouse (Université de Toulouse, CNRS, IRD), 14 avenue Edouard Belin, 31400 Toulouse, France*
[b] *Indo-French Cell for Water Sciences, Indian Institute of Science, Bangalore 560012, India*
[c] *Centre de Recherches Hydrologiques, P.O. Box 4110, Yaoundé, Cameroon*
[d] *INRA Agrocampus Rennes, UMR, Sol-Agronomie-Spatialisation, 65 rue de St Brieuc, 35042 Rennes, France*

Received 21 October 2013; accepted in revised form 7 September 2014; available online 28 September 2014

Abstract

The proportion of chemical elements passing through vegetation prior to being exported in a stream was quantified for a forested tropical watershed (Mule Hole, South India) using an extensive hydrological and geochemical monitoring at several scales.

First, a solute annual mass balance was established at the scale of the soil–plant profile for assessing the contribution of canopy interaction and litter decay to the solute fluxes of soil inputs (overland flow) and soil outputs (pore water flow as seepages). Second, based on the respective contributions of overland flow and seepages to the stream flow as estimated by a hydrological lumped model, we assigned the proportion of chemical elements in the stream that transited through the vegetation at both flood event (End Member Mixing Analysis) and seasonal scales.

At the scale of the 1D soil–plant profile, leaching from the canopy constituted the main source of K above the ground surface. Litter decay was the main source of Si, whereas alkalinity, Ca and Mg originated in the same proportions from both sources. The contribution of vegetation was negligible for Na. Within the soil, all elements but Na were removed from the pore water in proportions varying from 20% for Cl to 95% for K: The soil output fluxes corresponded to a residual fraction of the infiltration fluxes. The behavior of K, Cl, Ca and Mg in the soil–plant profile can be explained by internal cycling, as their soil output fluxes were similar to the atmospheric inputs. Na was released from soils as a result of Na-plagioclase weathering and accompanied by additional release of Si. Concentration of soil pore water by evapotranspiration might limit the chemical weathering in the soil. Overall, the solute K, Ca, Mg, alkalinity and Si fluxes associated with the vegetation turnover within the small experimental watershed represented 10–15 times the solute fluxes exported by the stream, of which 83–97% transited through the vegetation. One important finding is that alkalinity and Si fluxes at the outlet were not linked to the "current weathering" of silicates in this watershed.

These results highlight the dual effect of the vegetation cover on the solute fluxes exported from the watershed: On one hand the runoff was limited by evapotranspiration and represented only 10% of the annual rainfall, while on the other hand, 80–90% of the overall solute flux exported by the stream transited through the vegetation.

The approach combining geochemical monitoring and accurate knowledge of the watershed hydrological budget provided detailed understanding of several effects of vegetation on stream fluxes: (1) evapotranspiration (limiting), (2) vertical transfer through vegetation from vadose zone to ground surface (enhancing) and (3) redistribution by throughfalls and litter decay. It provides a good basis for calibrating geochemical models and more precisely assessing the role of vegetation on soil processes.

* Corresponding author at: Géosciences Environnement Toulouse (Université de Toulouse, CNRS, IRD), 14 avenue Edouard Belin, 31400 Toulouse, France.
E-mail address: jean.riotte@get.obs-mip.fr (J. Riotte).

http://dx.doi.org/10.1016/j.gca.2014.09.015
0016-7037/

1. INTRODUCTION

Solute-based geochemical mass balance methods are widely used in small experimental watersheds (SEW) to assess (i) the relative contribution of chemical weathering flux to the overall outlet flux (Paces, 1983) and (ii) the weathering rates of primary and secondary minerals (Velbel and Price, 2007; Price et al., 2012). The role of biota, including vegetation, soil microorganisms (e. g. bacteria, fungi) and soil engineers (e. g. earthworms, termites) is increasingly recognized to favor chemical weathering processes (Drever, 1994; Amundson et al., 2007; Gadd, 2007; Brantley et al., 2012a). However, the role of vegetation cycling on the solute output flux is still not well understood and quantified.

In forested ecosystems, elemental uptake by aggrading forest can act as a sink for some mineral-derived cations, whereas element release from the decaying forest biomass can result in enhanced solute fluxes (Velbel and Price, 2007, Price et al., 2012). Comparison of vegetated and non-vegetated systems, either experimentally or on paired watersheds, can also be used to decipher the effect of the plant cycling. Bormann et al. (1998), for instance, determined from input–output budgets in sand box ecosystems that aggrading vegetation enhances weathering rates by factors of 10 for Ca and 18 for Mg compared to non-vegetated sandboxes. Similarly, Moulton et al. (2000) reported that the release of Ca and Mg to Iceland streams was about 4 times higher in vegetated areas than in bare landscapes.

Besides processes favoring mineral breakdown and subsequent elemental release, vegetation cover generates evapotranspiration, and thereby controls water availability for surface runoff, infiltration and groundwater recharge in the ecosystem. Evapotranspiration is directly linked to the nature of the vegetation cover and the local climate. For a mean annual rainfall (P) below 700 mm yr^{-1}, evapotranspiration accounts for nearly 90% of the water budget in arid and semi-arid forests, and even with P of 3000 mm yr^{-1} or 1300 mm yr^{-1} in grasslands it still accounts for 50% of the water budget (Zhang et al., 2001). The main consequences of high evapotranspiration are (i) the decrease of the water–rock ratio and (ii) the concomitant increase of solute concentrations in percolating pore waters. This modifies the saturation indices and tends to slow down chemical weathering and limit the export of solutes (e.g. Braun et al., 2005, 2012; Chadwick and Chorover, 2001).

Understanding the impact of vegetation cover on solutes exported by streams needs to combine studies on both vegetation elemental cycling and water balance. This can be addressed by assessing input–output elemental mass balance at the soil–plant scale and then identifying the plant contribution to the stream flux. However, connecting observations at the vegetation/soil profile with solute fluxes exported from the stream requires, in addition to mineralogical and geochemical data, a thorough knowledge of water pathways and water fluxes within the SEW. Another way to quantify chemical weathering and biomass uptake was proposed by Rice and Price (2014). It consists of mass balance calculations on small forested watersheds underlain by relatively unreactive quartzite bedrock. Such unreactive bedrock and associated low chemical weathering rates offer the opportunity to quantify the biomass nutrient (K, Ca, Mg) uptake stoichiometry. This biomass stoichiometry can be further put into coefficient matrices, allowing the calculation of mineral chemical weathering rates (Bowser and Jones, 2002), and applied to small forested watersheds developed on reactive bedrocks (Price et al., 2013).

Since 2001, an integrated study has been carried out on the pristine SEW of Mule Hole (South India), developed on a granito-gneissic basement. This SEW, covered by a deciduous dry forest, is located in the sub-humid zone of the climatic gradient of the Western Ghats rain shadow and has been monitored since 2003 for climatic, hydrological and geochemical parameters (http://bvet.omp.obs-mip.fr/index.php/eng/). The SEW was characterized for (i) soil distribution and erosion processes (Barbiero et al., 2007), (ii) groundwater storage in the hard-rock aquifer (Legchenko et al., 2006), (iii) seasonal local recharge processes at the stream outlet (Descloitres et al., 2008), and (iv) spatial thickness, mineralogy and geochemistry of the regolith (Braun et al., 2009). More recent papers have specifically addressed water and geochemical cycles based on the combined use of several methods such as chloride mass balance, water table fluctuation, geophysics, groundwater chemistry and flow analysis (Maréchal et al., 2009; Parate et al., 2011; Maréchal et al., 2011). Hydrological lumped models simulating the water balance at the SEW scale have been developed to assess (i) the significance of the regolith vadoze zone in both water uptake by deep tree roots and groundwater recharge process (Ruiz et al., 2010), and (ii) weathering processes in combination with the forward geochemical model WITCH (Goddéris et al., 2006). The resulting hydrogeochemical model (Violette et al., 2010a) estimated the dissolution/precipitation rates of minerals using laboratory kinetic laws and was used as an exploratory tool for deciphering the geochemical processes which likely take place in the SEW. Mineral weathering rates and chemical fluxes at the SEW scale were also inferred by inverse modeling using the composition of the primary and secondary minerals and groundwater chemistry (Siva Soumya et al., 2011). However, none of these studies took into account the influence of elemental cycling through vegetation.

Given the specific conditions of the water balance in the Mule Hole SEW, including high evapotranspiration, low stream discharge, and disconnection between surface/subsurface and ground waters, it constitutes an ideal site to scrutinize how and to what extent elemental transfer within the vegetation cover participates in solute exports at the soil/plant scale and at the stream level. Based on the water fluxes calculated from the lumped hydrological numerical model of Violette et al. (2010a), the present study assesses the vegetation contribution to (i) chemical fluxes at the soil/plant scale, taking into account the elemental composition of atmospheric inputs, throughfall, overland flow water, and soil pore water; and (ii) chemical fluxes to the stream at the flood event scale, using the end member mixing analysis (EMMA), and at the yearly scale.

2. ENVIRONMENTAL SETTINGS

The Mule Hole SEW (4.1 km^2) is located 11°72′N and 76°42′E, in the sub-humid part of the climatic gradient of the Kabini river basin in the Southwest part of Peninsular India. Parent rocks, saprolite and soil cover are described in detail by Barbiero et al. (2007), Braun et al. (2009), Violette et al. (2010a, b) and Siva Soumya et al. (2011).

Parent rocks consist of peninsular gneiss intermingled with much less abundant mafic to ultramafic rocks, mostly amphibolite. Major minerals of the granito-gneiss are quartz, oligoclase, sericite, biotite and chlorite (Braun et al., 2009). The average thickness of the regolith in Mule Hole SEW is 17 m and consists of 15 m of immature saprolite and 2 m of topsoil (Braun et al., 2009). The saprolite mineralogy is composed of residual quartz, oligoclase, biotite, and chlorite crystals and secondary clays (goethite) and clay minerals (kaolinite, smectite).

The soil cover is mainly composed of a Ferralsol–Vertisol system (Barbiero et al., 2007; IUSS-Working-Group-WRB, 2006). Shallow Ferralsol (Ferralsols and Chromic Luvisols) from 1 to 2 m in depth dominate on the hillslopes (Fig. 1). An assemblage of secondary clays and clay minerals dominated by kaolinite and goethite characterizes their mineralogy. Residual crystals of quartz, sericite and, to a lesser extent, Na-plagioclase, from albite to oligoclase in composition, are preserved. The lower part of the hillslopes and flat valley bottoms are covered with, on average, 2 m of Vertisols and Vertic intergrades. Thicker Vertisols (2.5 m) also develop on amphibolite-rich bedrock located in the depressions on the crest line. The Vertisols are rich in smectite with shrink-swell potential. The mineralogy of the gneiss-derived Vertisols is dominated by smectite in the secondary clay assemblage and lower proportion of kaolinite and interstratified kaolinite-smectite. The Ferralsols cover 66% of the entire watershed area, the Vertisols 12% and the saprolite outcrops (shallow Ferralsols) 22% of the watershed.

The vegetation is a dry deciduous forest, dominated by the "ATT" facies, i.e. *Anogeissus latifolia* ((Roxb. ex DC.) Wall. ex Guillem. & Perr., *Tectona grandis* (*Tectona grandis* L.f.) and *Terminalia crenulata* (*Terminalia crenulata* Roth.) for trees and *Themeda triandra* (*Themeda triandra* Forssk.) (Elephant Grass) for grass (Fig. 1; Barbiero et al., 2007). This assemblage, developed on thick Ferralsol and shallow Vertisol, accounts for 70% of the watershed area. The remaining 30% consists of *Shorea* spec. trees, associated with well drained saprolite outcrops topped by shallow Ferralsol and *Ceriscoides* spec. trees, typical for Vertisols. Tree leaves in the SEW grow before the rainy season, during dry season. This is known as "the paradox of Asian monsoon forests" (e.g. Elliott et al., 2006). When the monsoon starts, litter fall has already occurred a few months before and fresh leaves have already grown. The stem density >1 cm

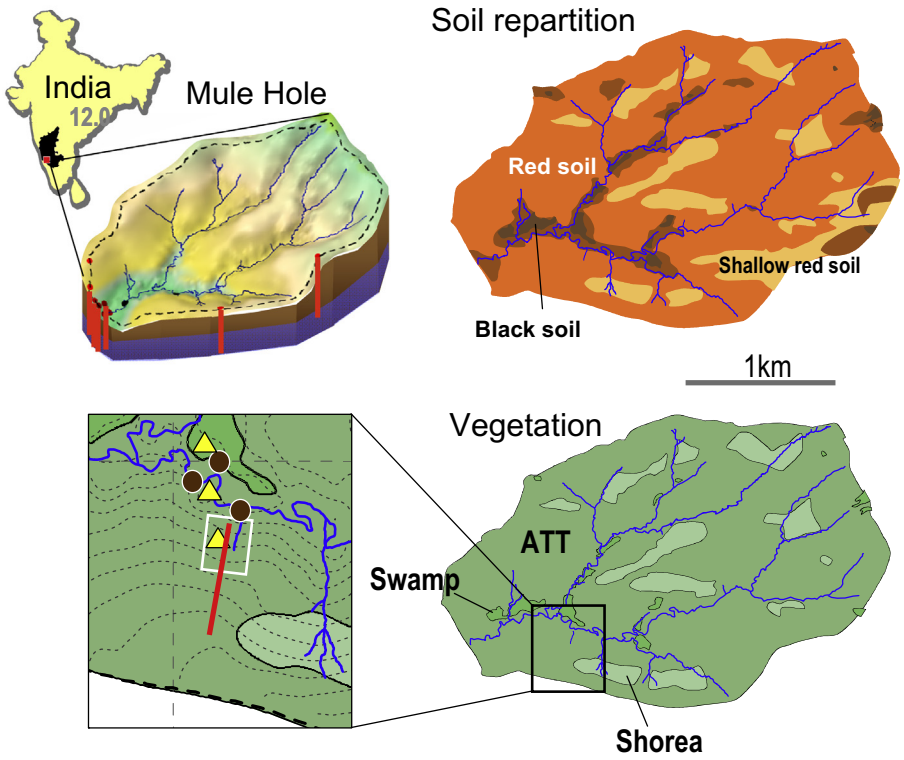

Fig. 1. The Mule Hole watershed with soil and vegetation maps (from Barbiero et al., 2007). ATT facies refers to *A. latifolia*, *T. grandis*, *T. crenulata* trees assemblage. The red line corresponds to the transect where litter was collected, the white rectangle to the throughfalls (TF) sampling area, yellow triangles to overland flows sampling (OF) and brown dots to seepage sampling locations. (For interpretation of the references to colour in this figure legend, the reader is referred to the web version of this article.)

dbh, determined in the Mudumalai forest in similar climatic conditions to Mule Hole, ranges from 250 to 500 stems/ha (Suresh et al., 2011).

The annual rainfall ranges from 700 mm yr^{-1} (e.g. year 2003) to 1500 mm yr^{-1} (e.g. year 2005) with an average of 1100 mm yr^{-1} over the last 30 years (data from the Karnataka Forest Department for the period 1975–1995 and from this team since 2003). Almost 90% of rainfall originates from the South-West Monsoon, active from June to October. Between 2004 and 2006, evapotranspiration accounted for 86% of the annual rainfall ($P =$ 1280 mm yr^{-1} for this period, Maréchal et al., 2009). Groundwater recharge, both direct (diffused at the hillside level) and indirect (through the stream channel), deduced from chlorine mass balance, accounted for only $6 \pm 2\%$ and runoff for $8 \pm 2\%$. The water balance at the Mule Hole SEW indicates that the forest (vegetation) limits both groundwater recharge and runoff. As a consequence, groundwater is disconnected from surface flow (Maréchal et al., 2009). The stream is then highly intermittent and flood events last from a few hours to a few days. Moreover, the chemical weathering fluxes exported by groundwater dominate over those of stream fluxes (Maréchal et al., 2011). The stream composition is a mixture of overland flow on Ferralsol and Vertisol, originating from the vicinity of the streambed as open space channels, and seepage flow. While overland flow occurs almost instantaneously as rain starts, seepage flow only occurs when the Ferralsol soil layer is saturated, during the second part of the rainy season. It can seep for a few days following the rainy event. Few channel pipe flows were observed in the notch of the streambed. The stream channel follows the limits of Vertisol patches in the valley bottoms.

3. MATERIALS AND METHODS

3.1. Water sampling and chemical analyses

The geochemical monitoring of the watershed, initiated in 2003, consists of collecting time-series of water samples at an hourly level for floods, daily for rainfall events, and monthly for groundwater. The outlet was equipped with an auto-sampler (ISCO®) to collect water samples every 60 or 90 min during storm events ($n = 186$ between 2005 and 2009). For each rainfall event ($n = 250$ between 2003 and 2010), open field deposits were collected in open polyethylene bags at the Mule Hole check-post, 1 km away from the outlet of the watershed. Open bag collection integrates both wet deposits and the coarse, gravitationally settled fraction of dry deposits. In addition, water samples of throughfall, overland flow and soil seepage flow were collected. The throughfall samples ($n = 29$) were collected in polyethylene bags in September 2009 during a single rainfall event at the Mule Hole SEW below trees of the ATT facies, below few other tree species, and also below *T. triandra* and shrub, in order to assess species-related variability of rainfall interaction with canopy, shrub and grass and to estimate the possible contribution of fine dry deposits. The overland flow samples ($n = 20$) were collected from 2009 to 2011 to assess the intensity of litter leaching and characterize the composition of water infiltrating into the soil layer. Two home-made samplers, consisting in a PVC pipe filled with plastic mesh, were laid on the ground surface in a gully where overland flow was previously observed. The pipe was connected with a Tygon® tube to a buried 5 L can. One sampler was placed on Ferralsol and the other on the transition between Vertisol and Ferralsol. The drainage area of each collector was approximately 100 m^2, ensuring short flow duration on the ground surface –typically few seconds- and hence a minimal interaction with surface soil minerals. Each sample collected in the can integrated a few weeks of ephemeral overland flow. In 2004, one water sample was collected in a swamp over a Vertisol. The soil seepage samples ($n = 11$) were collected along the Mule Hole stream channel close to the soil toposequence that served as a reference for soil studies in the SEW (Barbiero et al., 2007; Fig. 1) in 2004 for the Vertisol and in 2009 and 2010 for the Ferralsol/Vertisol transition.

Water samples were filtered in the laboratory (Sartorius® cellulose acetate, 0.22 μm membrane) and split into two aliquots and stored in PP bottles: One (acidified with bi-distilled HNO_3) for the determination of cation concentrations, the other (non-acidified) for the determination of anion concentrations. The non-acidified flask was stored in a refrigerator until anions and DOC were analysed. For samples collected from 2006 onwards, alkalinity was measured at the Indo-French Cell for Water Sciences (IFCWS), Indian Institute of Science, Bangalore, with an auto-titrator Mettler Toledo DL50Gx, while for samples collected earlier it was estimated from the anionic deficit. The systematic comparison of both the methods since 2006 provided consistent results. The other anions F^-, Cl^-, NO_3^-, PO_4^-, SO_4^{2-} were determined with an Ion Chromatograph Dionex DX600 (IFCWS, Bangalore). Cations of ground and surface waters were measured by atomic absorption spectroscopy or a Thermo ICP-OES at Geosciences Environment Toulouse (GET, France), whereas those of rainwater were measured by ICP-MS (Elan 6000, GET, France). Dissolved organic carbon (DOC) was measured with a Shimadzu TOC 5000 carbon analyzer (either GET, Toulouse or IFCWS, Bangalore). Procedure blanks (filtration and storage) were below 0.15 mg L^{-1} of DOC, which is negligible compared to the concentrations typically found in the water bodies of Mule Hole, apart from the most diluted rain samples. Procedure blanks for the other chemical species were at the level of detection limit of ion chromatograph and ICP-OES, i.e. <1 μmol L^{-1}. Silica was determined with a Hach spectrophotometer (IFCWS, Bangalore). The overall precision obtained for the concentration measurements were better than 10%. The reference materials used for the quality check was ION 915 or BMOOS (lake waters) for surface waters, and RAIN 97 for rain samples, all from National Research Water Institute, Canada.

3.2. Vegetation sampling and chemical analysis

Leaf and herbaceous litters were collected during the dry seasons of 2009 and 2010 from the dominant soil/vegetation configuration in the watershed, i.e. ATT vegetation developed on Ferralsol. A transect of 4 m by 260 m (i.e.

total area of 1040 m^2, Fig. 1) along the northern slope was selected, then divided into 13 segments of 4 by 20 m in which all the litter was collected. Herbaceous litter, mainly composed of *T. triandra* grass was harvested in January. *T. grandis* leaves were picked up separately whereas the remaining leaves -not identified- were collected from the ground in January and March. A sample of 5–10 kg of each herbaceous/leaf group was brought to the laboratory and dried at 70 °C to convert field data into dry weights. Although possibly less precise than a quantification from a large number of litter traps, this method was preferred as elephant herds are prone to destroy or remove any visible set up in the watershed. An advantage was to include the annual herbaceous litter production, which is significant in dry deciduous forests (Long et al., 1989; Suresh et al., 2011). A large dry sample (approx. 1 kg) of each major species, i.e. *A. latifolia*, *T. grandis*, *T. crenulata*, *T. triandra* and two samples of mix (remaining) leaves were stored for further chemical analyses.

The dry litter samples were powdered with an agate mortar. The carbon concentration was measured on a 50-mg aliquot using a Horiba Emia-320V carbon–sulphur analyzer. Another 100 mg aliquot was digested with HNO_3, HF and H_2O_2 in a Mars Express microwave oven for cation analysis by ICP-OES. Finally, a last aliquot of 100 mg was digested with HNO_3 and H_2O_2 and centrifuged to isolate phytoliths. The phytoliths were dissolved in hot NaOH and then mixed with the supernatant for analysis of silica by ICP-OES. All species were analyzed twice or three times to ensure the representativeness of chemical compositions.

3.3. Data handling

3.3.1. Modeling of hydrological fluxes

The lumped hydrological model developed for the Mule Hole watershed (Violette et al., 2010a) was modified to consider canopy interception and the long-term average rainfall of 1100 mm yr^{-1}. This is a reservoir model designed to simulate on an hourly basis the water storage on canopy leaves, in soil, in saprolite and the exchange flows between these reservoirs. The forcing parameters are rainfall (P) measured by the meteorological station and potential evapotranspiration (PET). The total actual evapotranspiration (AET) is computed from the canopy interception (Inter), the soils (Ep) and saprolite (Ea) according to available water with the following equation:

$$\mathrm{AET} = \mathrm{Inter} + \mathrm{Ea} + \mathrm{Ep} \leqslant \mathrm{PET} \tag{1}$$

This provides a way to consider deep root water uptake by the forest. This triple-box model was replicated for Ferralsol and Vertisol profiles. At the scale of the watershed, the water balance can be described as:

$$P = \mathrm{AET} + Q_{\mathrm{stream}} + \mathrm{R} \tag{2}$$

with Q_{stream} the stream flow and R the groundwater recharge. Change in soil water stock was neglected at the annual budget scale. The total flows are weighted according to the respective surface areas of Ferralsol and Vertisol. The simulated runoff at the outlet, calculated as:

$$Q_{\mathrm{stream}} = Q_{\mathrm{OF}} + Q_{\mathrm{seepage}} \tag{3}$$

was used for the model calibration, with Q_{OF} the flux from the overland flow and Q_{seepage} the flux from the soil layer (inter flow). The flow to the aquifer was constrained to match with yearly estimates of the total recharge obtained from the chloride mass balance method for the period 2004–2006 (Maréchal et al., 2009). The water budget at the scale of 1D soil–plant profile can be described as:

$$P = \mathrm{Inter} + Q_{\mathrm{ground}} \tag{4}$$

where $Q_{\mathrm{ground}} = Q_{\mathrm{OF}} + Q_{\mathrm{soil\ input}}$ and $Q_{\mathrm{soil\ input}}$ is the water flux infiltrating into the soil layer. Within the soil, part of this flux can be evaporated (Ep), the other ($Q_{\mathrm{soil\ output}}$) leaves the soil towards the stream (Q_{seepage}) or towards the saprolite ($Q_{\mathrm{saprolite}}$):

$$Q_{\mathrm{soil\ input}} = Q_{\mathrm{soil\ output}} + \mathrm{Ep} = Q_{\mathrm{seepage}} + Q_{\mathrm{saprolite}} + \mathrm{Ep} \tag{5}$$

3.3.2. Solute mass balance at the soil–plant profile scale

3.3.2.1. Chemical fluxes to the ground surface. For a given element X, the contribution of vegetation cycling to the chemical flux reaching the ground surface before infiltrating the soil layer is defined by:

$$F_{\mathrm{X\ vegetation\ cycling}} = F_{\mathrm{X\ ground}} - F_{\mathrm{X\ atm\ inputs}} \tag{6}$$

The contribution of vegetation as leachates occurs at two levels: (1) interaction with the canopy (leaching and uptake from leaves) and (2) interaction with dry litter at the ground surface, further referred as "litter leaching". The net atmospheric input flux is given by the following equation:

$$F_{\mathrm{X\ atm\ inputs}} = F_{\mathrm{X\ open\ field}} + F_{\mathrm{X\ dry\ deposits}} \tag{7}$$

With open field deposits expressed as:

$$F_{\mathrm{X\ open\ field}}(\mathrm{mol\,ha^{-1}\,yr^{-1}}) = \frac{C^{\mathrm{VWM}}_{\mathrm{X\ open\ field}}(\mu\mathrm{mol\,L^{-1}}) \cdot \mathrm{P(mm\,yr^{-1}})}{100} \tag{8}$$

where $C^{\mathrm{VWM}}_{\mathrm{X\ open\ field}}$ is the volume weighted mean concentration of the element X in the rainfall events and P is the annual rainfall amount. In this study dry deposits were not directly measured. Their contribution was assessed using a tracer ion and the throughfall composition. Among the tracers tested in previous studies, Na, Cl, SO_4 and Ca (see Staelens et al., 2008 for a review), Na was found to be the most inert. As it is widely used from tropical to boreal forests, Na was also chosen for estimating the dry deposit fraction in Mule Hole using the equation (adapted from Staelens et al., 2008):

$$F_{\mathrm{X\,dry\,deposits}} = \left(\frac{C^{\mathrm{M}}_{\mathrm{Na\ throughfall}} - C^{\mathrm{VWM}}_{\mathrm{Na\ openfield}}}{C^{\mathrm{VWM}}_{\mathrm{Na\ openfield}}} C^{\mathrm{VWM}}_{\mathrm{X\ open\ field}} \right) \cdot \frac{P - \mathrm{inter}}{100} \tag{9}$$

with the same units as in the previous equation. When precipitation passes through the canopy, the fraction that is not intercepted by canopy becomes throughfall and the flux associated can be written as follows:

$$F_{\mathrm{X\ throughfall}} = F_{\mathrm{X\ atm\ inputs}} + \Delta F_{\mathrm{X\ canopy\ interaction}} \tag{10}$$

$$F_{X\ throughfall}(\text{mol ha}^{-1}\ \text{yr}^{-1}) = \frac{C_{X\ throughfall}(\mu\ \text{mol L}^{-1}) \cdot (P - inter)(\text{mm yr}^{-1})}{100} \quad (11)$$

where $C_{X\ throughfall}$ is the average concentration of the element X in throughfall and (P – inter) the non-intercepted rainfall flux. The net contribution of canopy interactions, i.e. net throughfall, ($F_{X\ canopy\ interaction}$) is assessed by:

$$\Delta F_{X\ canopy\ interaction} = F_{X\ canopy\ exudates} - F_{X\ canopy\ uptake} = F_{X\ throughfall} - F_{X\ atm\ inputs} \quad (12)$$

When precipitation reaches the ground, the short interaction with decaying litter adds an additional contribution from vegetation, $F_{X\ litter\ leaching}$. For any element X, the chemical flux to the ground can be expressed by:

$$F_{X\ ground} = F_{X\ atm\ inputs} + \Delta F_{X\ canopy\ interaction} + F_{X\ litter\ leaching} \quad (13)$$

Assuming that the chemical composition of the overland flow collected close to the stream reflects the composition of the water reaching the ground surface in the entire watershed, the solute flux of an element X to the ground can then be assessed by:

$$F_{X\ ground}(\text{mol ha}^{-1}\ \text{yr}^{-1}) = k \cdot \frac{C_{X\ overland\ flow}(\mu\ \text{mol L}^{-1}) \cdot Q_{ground}(\text{mm yr}^{-1})}{100} \quad (14)$$

where $C_{X\ overland\ flow}$ is the average concentration of the element X in overland flow, and k is the evaporation factor between throughfall and overland flow. The chemical flux from litter leaching is:

$$F_{X\ litter\ leaching} = F_{X\ ground} - F_{X\ atm\ inputs} - F_{X\ canopy\ interaction} \quad (15)$$

Or

$$F_{X\ litter\ leaching} = F_{X\ ground} - F_{X\ throughfall} \quad (16)$$

Grouping the canopy interaction and litter leaching fluxes into a single term, $F_{X\ vegetation\ cycling}$, the flux of element X that cycled through the vegetation in fluxes to the ground is expressed as:

$$F_{X\ vegetation\ cycling} = F_{X\ ground} - F_{X\ atm\ inputs} \quad (17)$$

And its relative proportion in the fluxes to the ground is:

$$f_{vegetation\ cycling\ to\ ground} = \frac{F_{X\ vegetation\ cycling}}{F_{X\ ground}}(\%) = 100 \cdot \left(1 - \frac{F_{X\ atm\ inputs}}{F_{X\ ground}}\right) \quad (18)$$

If $F_{X\ ground} = F_{X\ atm\ inputs}$, the element X is not influenced by cycling through the vegetation: it can be considered as conservative above the ground surface.

3.3.2.2. Chemical fluxes within the soil. The net chemical flux from the soil is defined by:

$$\Delta F_{X\ soil} = F_{X\ soil\ output} - F_{X\ soil\ input} \quad (19)$$

If $\Delta F_{X\ soil} < 0$ the soil layer is a sink for X, possibly due to the formation of secondary phases, adsorption and/or root uptake (e.g. White and Blum, 1995; Moulton et al., 2000). In this case, the soil output of X corresponds to a fraction of the soil input of X and it can be considered that $F_{X\ soil\ output}$ originates from both atmospheric inputs and vegetation cycling in same proportions as in $F_{X\ ground}$ ($f_{vegetation\ cycling\ from\ soil} = f_{vegetation\ cycling\ toground}$). If $\Delta F_{Xsoil} = 0$, X exhibits a conservative behavior. If $\Delta F_{Xsoil} < 0$, there is a net production of element X by the soil layer, possibly due to dissolution of primary or secondary phases or desorption. The fraction of element X produced by the soil layer would be:

$$f_{weathering}(\%) = \frac{F_{X\ soil}}{F_{X\ soil\ input}} \cdot 100 \quad (20)$$

And the fraction of X that transited through the vegetation in the soil output, inherited from infiltration, would be:

$$f_{vegetation\ cycling,\ soil\ output}(\%) = (1 - f_{weathering}) \cdot f_{vegetation\ cycling\ to\ ground} \cdot 100 = \frac{1 - F_{X\ soil}}{F_{X\ soil\ input}} \cdot \frac{F_{X\ vegetation\ cycling}}{F_{X\ ground}} \cdot 100 \quad (21)$$

Then, the fraction of X from atmospheric inputs in the soil output, inherited from infiltration can be described as:

$$f_{atmosphere,\ soil\ output}(\%) = (1 - f_{weathering}) \cdot (1 - f_{vegetation\ cycling\ to\ ground}) \cdot 100 \quad (22)$$

The solute mass balances within the Ferralsol and Vertisol layers were assessed assuming that the chemical compositions of overland flows and seepages for each soil system were representative of the chemical compositions of the soil inputs and outputs, respectively. The input fluxes to Ferralsol or Vertisol are:

$$F_{X\ soil\ input}(\text{mol ha}^{-1}\ \text{yr}^{-1}) = \frac{C_{X\ overland\ flow}(\mu\ \text{mol L}^{-1}) \cdot Q_{soil\ input}(\text{mm yr}^{-1})}{100} \quad (23)$$

with $C_{X\ overland\ flow}$ the average concentration of the element X in overland flow and Q_{INPUT} the input water flux to the soil. The soil output fluxes are:

$$F_{X\ soil\ output}(\text{mol ha}^{-1}\ \text{yr}^{-1}) = \frac{C_{X\ seepage}(\mu\ \text{mol L}^{-1}) \cdot Q_{soil\ output}(\text{mm yr}^{-1})}{100} \quad (24)$$

with $C_{X\ seepage}$ the average concentration of the element X in seepages and $Q_{soil\ output}$ the output water flux from the soil.

3.3.3. Annual chemical fluxes at the outlet of the watershed

At the outlet of the watershed, the stream is fed by the overland flows on Ferralsol and Vertisol and the seepages from the Ferralsol whose chemical compositions were characterized in the soil plant mass balance (Violette et al., 2010a):

$$F_{\text{stream}} = F_{\text{OF Ferralsol}} + F_{\text{OF Vertisol}} + F_{\text{Seepage Ferralsol}} \quad (25)$$

The flux of an element X in the stream is expressed as:

$$F_{\text{X discharge}}(\text{mol ha}^{-1}\,\text{yr}^{-1}) = \frac{C^{\text{VWM}}_{\text{X stream}}(\mu\text{mol L}^{-1}) \cdot Q_{\text{stream}}(\text{mm yr}^{-1})}{100} \quad (26)$$

where $C^{\text{VWM}}_{\text{X stream}}$ is the volume-weighted mean concentration of element X in the stream ($n = 184$ between 2005 and 2009) and Q_{stream} the annual discharge of the stream.

3.4. Element origin at the flood event scale using EMMA

End-member mixing analysis (EMMA) was used to determine the proportions of end-members contributing to streamflow at the outlet of the Mule Hole SEW at the flood event level, following the procedure of Christophersen and Hooper (1992). Streamflow samples and end-members were standardized for all conservative tracers using the mean and standard deviation of streamflow following the procedure of Burns et al. (2001) and described in detail in Maréchal et al. (2011). A dataset was built for each hydrological year from the dissolved concentrations of Na, K, Ca, Mg, Cl and Si measured in the streamflow samples. It was then standardized into a correlation matrix such that element concentrations with greater variation would not exert more influence on the model than those with lesser variation (SO_4 for example). A principal-components analysis (PCA) was performed on the correlation matrix. Then, the compositions of four possible end-members, rainwater average, throughfall average, soil pore water average, and overland flow water, were standardized and projected into the U space defined by the stream PCA by multiplying the standardized values by the matrix of eigenvectors. The outliers of EMMA have been corrected, forcing the resulting fraction to zero and resolving other fractions by the geometrical approach described in Liu et al. (2004). The goodness-of-fit of solute concentrations predicted by the EMMA was compared with the concentrations measured during the storms through least-squares linear regression. The EMMA model

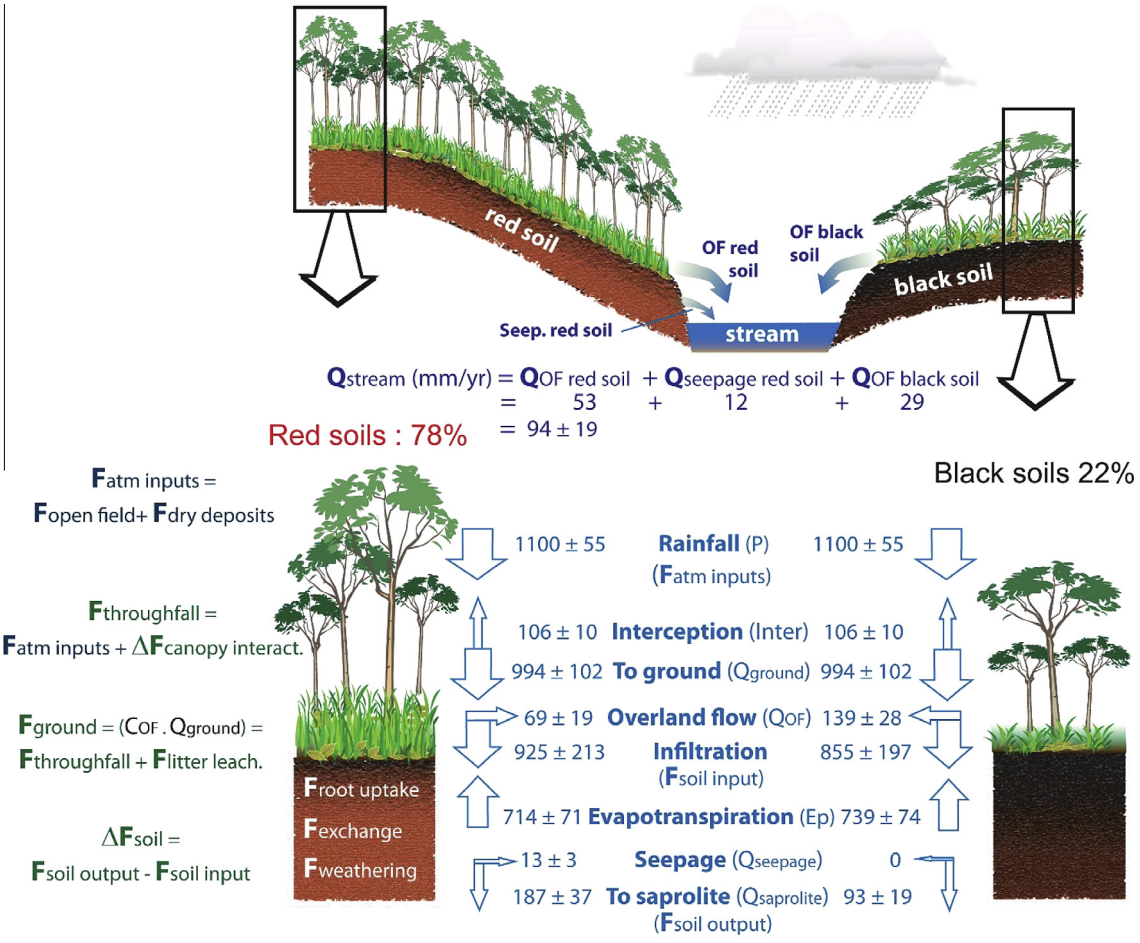

Fig. 2. Water budget (in mm yr^{-1}) of Mule Hole using long term average rainfall (1100 mm yr^{-1}, See Violette et al., 2010a) and processes affecting water and chemical fluxes at the vegetation-soil profile scale. Error margins are 5% for rainfall (uncertainty on rain gauge), 20% for stream flow (uncertainty on discharge calibration curve), 20% on recharge (from Maréchal et al., 2009, indirect recharge), 10% on evapotranspiration and interception (from Maréchal et al., 2009, Indirect recharge). Other margins are calculated using uncertainty propagation theory.

was then used to calculate the proportion of stream water derived from each of the four end-members for each sample collected during storms.

4. RESULTS

4.1. Hydrological balance

The long term average rainfall value, $P = 1100$ mm yr^{-1}, used to run the hydrological model is close to the mean annual rainfall for the period 2005–2010, 1200 mm yr^{-1} (Fig. 2). According to Ruiz et al. (2010), about 10% of the 1100 mm yr^{-1} rainfall is intercepted by the canopy. Both hydrological budget and field observations at the Mule Hole SEW indicate that apart from the vicinity of the stream where some overland flows occur, the whole flux passing through the canopy infiltrates without significant evaporation. Then, on the hillslopes, the water balance can be reasonably computed on a 1D vertical profile. Evapotranspiration within the soil layer represented 80% and 89% of infiltration in Ferralsol and Vertisol, respectively. Apart from a small fraction flowing to the stream as seepage, the remaining soil output flux percolated down to the saprolite. The runoff measured at the outlet of the Mule Hole stream ranged from 23 mm (2008) to 179 mm (2005). The average stream runoff computed by the model represented 8.5% of the incident rainfall, i.e. 92 mm yr^{-1} (Fig. 2), matching the average runoff measured over the same period. Taking into account the surface areas represented by Ferralsol-saprolite and Vertisol in the watershed, the average stream runoff was mainly composed of Ferralsol seepage (10 mm yr^{-1}) and overland flow (53 mm yr^{-1}). Though extension of Vertisol is limited, its occurrence in valley bottom favored significant overland flow (29 mm yr^{-1}).

4.2. Chemical composition of water compartments

The average chemical compositions of all throughfall, overland flow and soil seepage samples and the weighted average chemical compositions of rainfall and stream flow samples are presented in Table 1 and in Fig. 3.

In the rain water, the concentration values for Na, Ca, Mg, SO_4, NO_3 and Cl were about 50% less and for K about 200% more than the values reported in the literature for rural areas of India (Kulshrestha et al., 2005) or in pristine humid forests of Western Ghats (Prakasa Rao et al., 1995). The concentration variability was low compared to the other compartments (Fig. 3). The average Na/Cl molar ratio was 0.85, close to that of seawater (0.86). In contrast, the average K/Cl, Ca/Cl and Mg/Cl molar ratios were higher than those of seawater, with average relative enrichments of 17, 53 and 3 times for K, Ca and Mg respectively. These enrichments were similar to those observed by Braun et al. (2005) in the forested tropical SEW of Nsimi (Cameroon), who attributed them to contribution of salts emitted by canopy.

In the throughfall, the average concentrations and the variability were much larger than in the rain for all chemical species except for Na, which exhibited consistently low concentrations (Fig. 3). The ranges of chemical concentrations varied with the vegetation species (Fig. 4); for instance, the highest K, Ca, Mg, Alkalinity and Cl concentrations were observed in *A. latifolia* throughfalls and the highest Si and DOC in *T. grandis* and/or *T. triandra* throughfalls. Concentrations of K in throughfall were positively correlated with Cl, Mg and alkalinity (Fig. 4).

In the overland flows, average concentrations and variability were close to those observed in throughfall except for DOC, Mg and most notably for Si which was one order of magnitude larger (Fig. 3). Remarkably, the average concentration of Na was similar to the weighted average of rainfall. Over the sampling period, the chemical compositions of overland flows over Ferralsol were not significantly different from those of overland flows over the Ferralsol–Vertisol transition or from the unique overland flow sample collected on Vertisol. Overall, there was no relationship between the chemical composition of the overland flows and the nature of the substratum.

In the soil pore water, chemical compositions were depleted in K and DOC, strongly enriched in Na and Si and moderately enriched in Alkalinity, Cl, Ca and Mg compared to overland flows (Fig. 3).

At the outlet, the stream waters exhibited chemical compositions close to the concentration ranges of overland flows, i.e., low Na concentrations and higher K, Ca, Mg, Cl and alkalinity (Fig. 3). However, at the end of the rainy seasons, the flood recessions exhibited compositions tending towards those of the soil seepages, i.e., higher Na concentration and slightly higher Si, Ca, Mg and alkalinity concentrations.

4.3. Solute mass balance at the scale of the soil–plant profile

Na and Cl in open field deposits were found to be consistent with values reported in tropical contexts, especially regarding the distance to the sea (Soumya et al. 2009). Flux values ranged between inland values (e.g. Lilienfein and Wickle, 2004; Braun et al., 2005) and near-coastal values (e.g. McDowell & Asbury, 1994; Chuyong et al., 2004) (Table 2). Dry deposits were estimated using Na as a conservative tracer in throughfall and, as reference rainfall composition, the rainfall events that occurred just before and during throughfall collection. Since throughfalls samples were collected during a single event, such calculations can only provide a rough estimation of dry deposits. Keeping in mind this limitation, dry deposits accounted for less than one percent of open field deposits (Table 2). For the reason mentioned above, net throughfall fluxes were not calculated. The solute fluxes to the ground were calculated from the computed water flux $Q_{ground} = 994$ mm yr^{-1} and the average composition of overland flows. Compared to atmospheric deposits, they exhibit enrichments in Cl, Si, K, Ca, Mg, DOC and alkalinity (Table 2). The Na flux to the ground is similar to the atmospheric inputs (−13%) if one considers the uncertainty on atmospheric deposits of 20% (Lindberg et al., 1986), whereas NO_3 and SO_4 fluxes were depleted compared to the atmospheric inputs by 43% and 49%, respectively.

Soil output fluxes were estimated separately for Vertisol and Ferralsol profiles and then at the watershed scale

Table 1
Weighted average composition of rainfall ($n = 250$) and 2005–2009 stream storms (data available *in extenso* at http://bvet.omp.obs-mip.fr/index.php/fre/presentation), and chemical composition of throughfall, overland flows and seepages at Mule Hole.

	Sampling date	pH	Conductivity	DOC	Alkalinity	Si	F	Cl	NO3	SO4	Na	K	Ca	Mg
			µS/cm	mg/L	µeq/L	µmol/L								
Rainfall (n = 250)														
Average	05/03 to 04/10	6.4	17	1.4	35	3	0.5	27	14	11	22	8	27	7
Min		5.5	2	0	0	0	0.0	0	0	0	0	0	1	0
Max		7.9	44	4	269	22	8.6	129	200	86	125	117	235	47
Stream storms														
Weighted average	2005			5.0	383	161		41		8	35	87	94	65
Weighted average	2006			8.7	614	269		69		3	96	113	166	95
Weighted average	2008			7.3	389	152		43		3	40	119	120	69
Weighted average	2009			6.9	624	155		41		5	40	154	130	60
Throughfall														
TF 4 Banian	2–4/09/09	6.2	51	14.0	181	65	6	117	0	14	51	218	74	37
TF 5 unknown	2–4/09/09	6.7	98	38	361	30	2	189	0	7	34	379	136	60
TF 6 Anogeissus	2–4/09/09	6.5	47	22	242	11	1	50	0	8	31	207	118	42
TF 7 Tectona	2–4/09/09	6.3	34	18.5	165	55	1	40	0	7	22	151	83	26
TF 8 Tectona	2–4/09/09	6.4	44	16.8	267	38	0	36	0	6	23	202	89	38
TF 9 Anog. Term. Shrub	2–4/09/09	6.5	96	58	410	20	1	117	0	7	37	472	236	131
TF 10 Terminalia	2–4/09/09	6.5	38	11.2	190	16	4	66	0	12	24	182	82	31
TF 11 HE + shrub	2–4/09/09	6.6	19	3.3	72	15	0	46	5	9	34	38	56	13
TF 12 HE + shrub	2–4/09/09	6.6	66	14.3	423	76	1	93	0	12	39	126	201	73
TF 13 Anogeissus	2–4/09/09	6.0	177	11.1	522	10	2	338	0	1	29	1017	253	217
TF 14 Tectona	2–4/09/09	6.2	22	15.0	103	37	1	44	1	11	32	60	79	18
TF 15 unknown	2–4/09/09	6.2	47	8.3	187	45	1	93	0	17	35	186	119	34
TF 16 Anogeissus	2–4/09/09	6.5	37	12.0	199	12	0	46	1	8	29	124	120	23
TF 17 Anogeissus + Tectona	2–4/09/09	6.7	53	31	293	23	1	49	1	8	24	265	97	32
TF 18 Anogeissus	2–4/09/09	6.4	53	24	252	15	1	66	1	7	31	278	149	51
TF 19 Anogeissus	2–4/09/09	6.5	50	14.2	200	9	1	61	2	7	29	237	126	32
TF 20 Tectona	2–4/09/09	6.6	40	1.7	179	44	1	47	4	8	31	164	98	30
TF 21 HE + Shrub + Term	2–4/09/09	6.6	23	7.0	97	26	0	50	9	9	32	32	84	26
TF 22 Terminalia	2–4/09/09	6.6	36	6.7	196	19	0	60	1	9	37	83	129	27
TF 23 Terminalia	2–4/09/09	6.6	47	14.1	242	22	0	70	0	9	34	114	162	39
TF 24 Anog + Term + tectona	2–4/09/09	6.6	28	15.4	151	20	1	47	1	9	30	95	83	18
TF 25 Tectona	2–4/09/09	6.3	35	46	154	34	2	74	1	11	31	146	85	23
TF 26 Anogeissus	2–4/09/09	6.4	92	12.8	369	43	2	200	1	14	32	477	206	78
TF 27 Shrub	2–4/09/09	6.5	47	6.9	242	32	1	119	1	15	36	160	76	43
TF 28 Tectona	2–4/09/09	6.3	23	130	110	13	1	52	6	11	48	57	64	17
TF 29 Anogeissus trunk	2–4/09/09	6.1	121	10.0	458	32	2	143	2	5	33	790	209	138
TF 30 HE + Shrub	2–4/09/09	6.5	66	21	563	42	0	93	2	9	39	115	81	42
TF 31 Anog + Term	2–4/09/09	7.0	98	6.5	619	47	2	114	3	16	38	318	313	59
TF 32 HE	2–4/09/09	6.1	17	12.5	71	24	0	40	7	6	32	26	50	15
Overland flow														
On red soil	02/09/09	6.97	47	7.0		193	3	30	13	1	18	109	131	60
On red soil	05/10/09	7.08	38.9	5.7	271	164	1.8	31	8	3	9	88	76	46
On red soil	11/11/09	6.52	31	5.9	241	184	2.7	16	3	1	6	79	56	40
On red soil	21/04/10	7.03	121	7.0	436	141	3.7	175	33	42	36	378	237	127
On red soil	28/04/10	6.5	43	9.0	289	216	2	31	1	3	18	85	97	50
On red soil	24/05/10	6.38	74.2	6.4	259	251	2	105	12	19	19	247	152	86
On red soil	06/09/10	6.48	59	12.9	458	304	n.m.	45	n.m.	n.m.	15	112	167	84
On red soil	05/10/10	7.26	53.9	10.8	402	237	2	49	13	4	10	97	149	69
On red soil	29/11/10	6.49	51.4	6.4		178	1.1	60	19	5.4	18	101	144	75
On red soil	25/04/11	5.94	34.3	7.5		125	1.2	39	6.3	4.3	20	111	85	49
On black to red soil transition	02/09/09	7.34	80	7.3		246	7	65	9	5	54	172	192	90
On black to red soil transition	16/10/09	6.94	57.2	6.9	365	223	3.7	45	19	8	12	132	113	65
On black to red soil transition	11/11/09	6.68	42	6.7	382	195	2.7	19	1	1	7	126	80	53
On black to red soil transition	21/11/09	7.64	38	5.4	243	166	5.1	44	6	5	35	95	59	42
On black to red soil transition	21/04/10	7.71	48.8	7.7	158	n.m.	3.6	113	0	13	11	151	104	54
On black to red soil transition	24/05/10	6.43	41.3	6.4	220	110	4	40	7	16	29	114	104	55
On black to red soil transition	28/04/10	6.6	51	8.2	294	233	3	44	21	4	21	118	114	57
On black to red soil transition	06/09/10	6.57	57	9.2	413	243	n.m.	59	n.m.	n.m.	17	133	154	71
On black to red soil transition	05/10/10	7.48	89.3	9.8	761	324	1	37	26	3	9	154	271	119

Table 1 (*continued*)

	Sampling date	pH	Conductivity	DOC	Alkalinity	Si	F	Cl	NO3	SO4	Na	K	Ca	Mg
			µS/cm	mg/L	µeq/L	µmol/L								
On black to red soil transition	29/11/10	6.4	64.1	6.8		217	0.8	66	4.6	2.3	27	120	190	89
On black soil	04/08/04	65	6.74	12.5	344	186	1	31	0	1	27	125	135	96
Soil Seepage														
Black soil 1	15/06/04	7.11	94	n.m.	470	368	1	69	0	5	143	119	249	107
Black soil 2	15/06/04	7.33	116	n.m.	645	405	3	57	0	1	101	197	332	144
Black soil 3	15/06/04	7.48	182	n.m.	1260	508	4	90	0	4	317	69	597	176
Black soil 4	15/06/04	7.3	218	n.m.	973	508	3	**326**	**175**	**69**	**630**	**32**	**488**	**224**
Red soil 1	23/07/09	7.6	89	7.5	242	349	7	76	13	3	276	7	11	13
Red soil 2	23–24/7/9	6.71	95	4.5	831	382	4	176	2	6	562	31	62	91
Red soil 3	23/07/09	7.45	94	9.7	807	401	6	217	2	3	634	26	56	84
Red soil 4	23/07/09	7.11	86	4.1	597	447	5	246	1	7	763	8	5	2
Red soil 5	11/11/09	7.19	74	5.0		n.m.	8.0	204	5	8	421	30	27	40
Red soil 6	30/11/10	7.33	59	6.8		451	n.m.	n.m.	n.m.	n.m.	409	40	58	40
Red soil 7	30/11/10	7.84	119	2.4		488	1	138	29	1	684	67	124	121

n.m. = not measured.

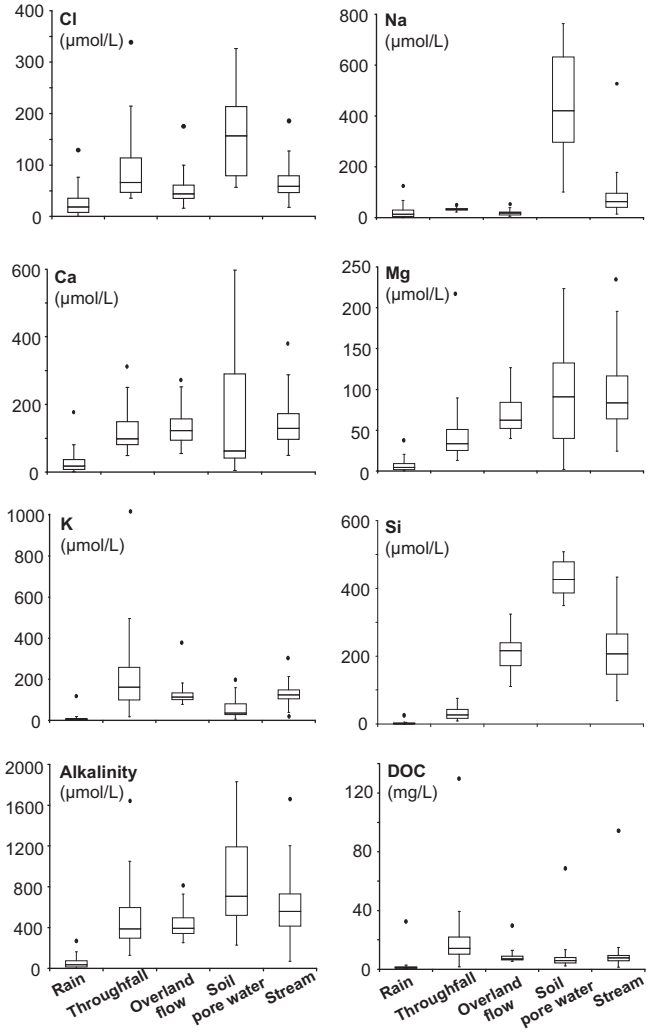

Fig. 3. Box plot showing the concentrations of major species in the various water bodies of the Mule Hole SEW (apart from groundwater): rainfall, throughfall, overland flow, pore water and stream.

according to the respective surface areas covered by each soil (Table 2 and Fig. 2). Soil output fluxes of Cl, K, Ca, Mg, Si were depleted compared to the inputs fluxes. In Ferralsols, the depletion followed the order Cl (33%) < Si (59%) < Mg (84%) < Ca (93%) < K (96%). In Vertisols, the depletion follows the order Cl (52%) < Ca (67%) < Si (74%) < Mg (81%) < K (91%). Sodium is the only element that exhibited a soil output flux higher that input flux, i.e., a net production from the soil layer, with large variations between Ferralsol (+450%) and Vertisols (+20 %). At the watershed scale, the soil outputs of K, Ca, Mg and Cl were similar to the atmospheric inputs.

4.4. Dry litter composition and budget (leaves and herbs)

The litterfall fluxes and the chemical compositions of leaves from the main tree species, from the unidentified leaf litter and from the main grass species are given in Table 3. Sodium concentrations in litter samples were below the ICP-OES detection limit, except for the mixed leaves with Na concentration of 0.018%. Calcium and Magnesium concentrations were the lowest in *T. triandra* grass and the highest in unidentified leaves and *T. crenulata* leaves. Potassium displayed a different pattern with lowest concentrations in leaves and highest in grass. Silica-bearing species consisted mainly of *T. triandra* and *T. grandis*. Carbon concentrations were homogeneous and consistent with the composition of cellulose (44.4%) and with values commonly found in leaves of tropical tree species (e.g., Fonseca et al., 2011).

The standard deviations associated with the litterfall fluxes correspond to the variability found among the thirteen subsections collected. The specific dry weights of *T. grandis* leaves and *T. triandra* grass, both hand-picked, remained stable between 2009 and 2010. The amount of other (mixed) leaves decreased, possibly due to inter-annual variability, or to a sampling artifact: as the ground surface was not cleaned in 2008, the higher amount found in 2009 may have included a residue of the previous year.

The estimates of total leaf litter production (Table 3) fell within the range compiled by Jaramillo et al. (2011) for dry tropical forests, from 2400 to 5500 kg ha^{-1}, and by Singh and Singh (1991) for Indian dry forests, from 3420 to 4700 kg ha^{-1}. The variation in the values obtained by different studies could be attributed to the different methods used for collecting the leaves.

The Ca and Mg fluxes associated with dry litter were almost entirely attributed to leaves (95% and 86%), while

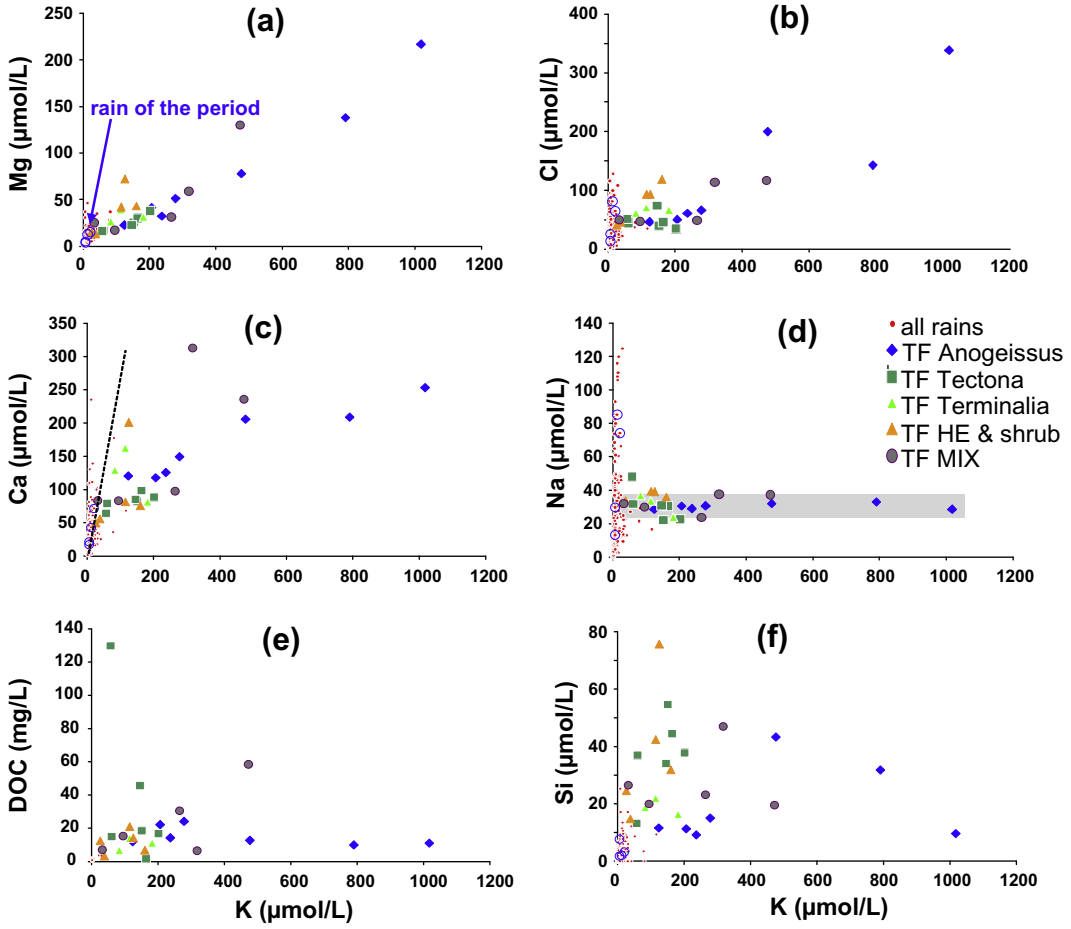

Fig. 4. Chemical composition of throughfall, species by species, compared to the rainfall composition: (a) Mg vs K, (b) Cl vs K, (c) Ca vs K, (d) Na vs K, (e) DOC vs K and (f) Si vs K. Species dependent trends are observed between K – used as a proxy of leaf exudates – and Ca, Mg and Cl. Na concentrations are remarkably constant among samples.

Table 2
Solute mass balance at the scale of a 1D soil-plan profile, in Ferralsol and Vertisol profiles and weighted average at the watershed scale.

	Water	DOC	Alkalinity	Si	F	Cl	NO3	SO4	Na	K	Ca	Mg
	(mm/yr)	g/ha/yr	eq/ha/yr	mol/ha/yr								
Above the ground												
Open field deposits	$P = 1100$	$F_{X\ \text{open field}} = 1250$	367	37	5	296	151	121	242	92	290	75
Dry deposits (Na inert)*	$Q_{\text{ground}} = \text{P-inter} = 994$	$F_{X\ \text{dry deposits Na}} = 0$	−4	0	0	−3	0	−1	−3	−1	−2	−1
Flux at ground surface	$Q_{\text{ground}} = \text{P-inter} = 994$	$F_{X\ \text{ground}} = 7219$	4179	2018	24	499	86	62	210	1328	1333	745
Vegetation cycling		$F_{X\text{vegetation cycling}} = 5969$	3812	1982	19	203	−64	−59	−32	1237	1043	669
Within ferrasol												
Input**	$Q_{\text{ferralsol input}} = 925$	$F_{X\ \text{ferralsol input}} = 5895$	4088	1923	26	515	103	71	181	1259	1237	639
Output	$Q_{\text{ferralsol output}} = 187$	$F_{X\ \text{ferralsol output}} = 961$	939	785	11	344	9	10	1001	56	92	104
Balance***	−738	$\Delta F_{X\ \text{ferralsol}} = -4934$	−3149	−1139	−15	−171	−94	−62	821	−1203	−1146	−535
Balance %	−80	−84	−77	−59	−58	−33	−92	−86	454	−96	−93	−84
Within vertisol												
Input**	$Q_{\text{vertisol input}} = 855$	$F_{X\ \text{vertisol input}} = 8906$	2941	1588	7	262	0	8	229	1069	1157	817
Output	$Q_{\text{vertisol output}} = 93$	$F_{X\ \text{vertisol output}} =$	1247	416	3	126	41	18	277	97	387	152
Balance***	−762	$\Delta F_{X\ \text{vertisol}} =$	−1695	−1172	−5	−136	41	10	48	−972	−770	−665
Balance%	−89		−58	−74	−61	−52		135	21	−91	−67	−81
*Winthin average soil***												
Input	$Q_{\text{soil input}} = 910$	$F_{X\ \text{soil input}} = 6558$	3836	1850	22	459	80	57	191	1217	1220	678
Output	$Q_{\text{soil output}} = 166$	$F_{X\ \text{soil output}} = 750$	1007	704	9	296	16	12	842	65	157	115
Balance***	−743	$\Delta F_{X\ \text{soil}} = -5808$	−2829	−1146	−13	−164	−65	−46	651	−1152	−1063	−563
Balance %	−82	−89	−74	−62	−59	−36	−81	−80	340	−95	−87	−83

* The rainfall values used for the calculation correspond to the period of TF sampling.
** *P*-Interception-OF: Rainfall minus interception minus overland flow.
*** The balance of water flow corresponds to the real evapotranspiration into soils profile.
**** Rates at the watershed scale (4.1 km^2) weighting ferralsol (78%) and vertisol (22%) contributions.

Table 3
Litter production and composition in 2009 and 2010. *A. latifolia* and *T. crenulata* leaves could not be separated in the mixture of leaves; their composition is given for comparison.

Composition (mol kg^{-1})	C	Na	Ca	Mg	K	Si
T. triandra (Elephant grass)	35.8	<dl	0.082	0.041	0.295	0.669
T. grandis leaves	36.7	<dl	0.474	0.171	0.152	0.701
A. latifolia leaves	35.8	<dl	0.80	0.111	0.148	0.014
T. alata leaves	33.3	<dl	0.686	0.189	0.172	0.142
Other leaves (mix)	35.0	0.005	0.985	0.103	0.082	0.169

Flux	Dry mass	C	Na	Ca	Mg	K	Si
	kg ha^{-1}	mol ha^{-1}	mol ha^{-1}	mol ha^{-1}	mol ha^{-1}	mol ha^{-1}	mol ha^{-1}
2009 Herbs	1663	6.0×10^4	<dl	136	67	490	1115
T. grandis leaves	1087	4.0×10^4	<dl	515	186	165	765
other leaves (mix)	2905	10.3×10^4	6	2862	300	239	493
Total	5654	20.3×10^4	6	3513	554	894	2372
Std %*	33			35	39	32	40
2010 Herbs	1538	5.5×10^4	<dl	125	62	453	1031
T. grandis leaves	1145	4.2×10^4	<dl	543	196	174	806
Other leaves (mix)	1693	6.0×10^4	3	1668	175	139	287
Total	4376	15.7×10^4	3	2336	433	767	2124
Std %*	14			21	27	11	24

* Standard deviation corresponding to the spatial variability over the 13 sampled subsections (4 × 20 m each).

60% of K was located in *T. triandra* grass. *T. triandra* and *T. grandis* leaves brought 80% to 85% of the silica flux. The Ca, Mg and K fluxes were very close to the values obtained for other tropical dry forests, such as those in Mexico (Campo et al., 2000). The litter-associated silica flux was slightly higher than that reported for vegetation developed on Ferralsols in Amazonia (Lucas, 2001, and reference therein). Given the absence of measurable Na in specific tree leaf species, the low Na concentration detected in the mixed leaves may correspond to a slight contamination by soil minerals (albite) and accordingly was neglected in the chemical mass balances discussed below.

4.5. End-member mixing analysis

EMMA was carried out on the stream chemistry at the outlet of the watershed during several flood events from 8 to 26th October 2008. The elements used in the EMMA were

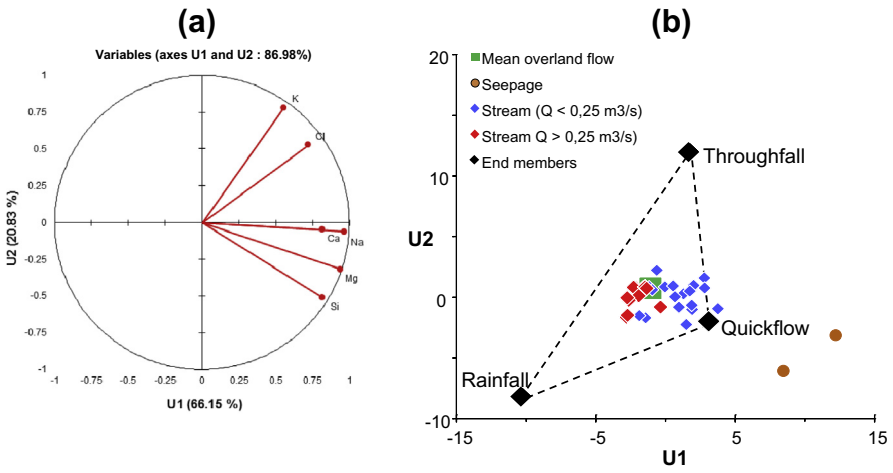

Fig. 5. (a) principal component analysis on 30 stream samples with projection on the main components. The first component (U1), explains 66% of the variance, with strong correlation (>0,75) with Na, Ca, Mg and Si solutes. The second component (U2), explains 21% of the variance and correlation between K and Cl; (b) Projection of the stream chemical composition in the U space after principal-components analysis (PCA) (blue and red diamonds). The compositions of four possible end-members, rainfall average, throughfall average, soil seepage average (brown dots) and overland flow (green square), are also projected. A quick flow component, mixture of overland flow and seepage, can be defined (see text). (For interpretation of the references to colour in this figure legend, the reader is referred to the web version of this article.)

Si, K, Mg, Na, Ca and Cl. The principal component analysis on 30 samples resulted in two significant components explaining 87% of the variance. This indicates that the chemical variation in stream water can be accounted for by three end-members. The first component (U1), explaining 66% of the variance, showed a strong correlation (>0.75) with Na, Ca, Mg and Si solutes. The second component (U2), explaining an additional 21% of variance, was correlated with Cl and strongly correlated with K (Fig. 5a). To simplify, the U1 axis can be considered as the mineralization axis (due to both soil and/or litter leaching) while the U2 axis is an indicator of canopy leaching. Tracer compositions of streamflow samples, plotted along with potential end-members in U space (Fig. 5b), allowed us to distinguish high flow conditions (discharge at the outlet $Q > 0.25\ m^3\ s^{-1}$) from low flow conditions ($Q < 0.25\ m^3\ s^{-1}$). The mean overland flow water concentration used for budget assessment is located on the U diagram in the middle of the stream water data cloud during high flow periods of October 2008, which confirmed that the overland flow component dominated other contributions during the storm. However, fluctuations in stream water chemistry around the overland flow end-member suggest a varying origin of the overland flow. Hence, the stream water can be bound by the following three end-members: rainfall, throughfall, and stream water (quickflow) collected eight hours after the peak of 26th October 2008 ($Q = 0.12\ m^3\ s^{-1}$), located on the U diagram between overland flow and seepage water, suggesting a composition close to a mixing of both of these end-members (Fig. 5b). The seepage end-member was also tested but it was not able to explain the stream chemistry during this flood event. During low flow conditions, the stream water tended towards the quickflow and seepage end-members. These results are in agreement with the hydrological model results which identified overland flow as the main component during high flow conditions while seepage appeared during recession periods.

5. DISCUSSION

5.1. Estimation of vegetation cycling at the soil–plant profile scale

5.1.1. Above the ground

At the soil–plant scale, vegetation mostly impacts solute mass balance by transferring chemical elements from the soil or saprolite to the ground surface via throughfall and litter decay. At Mule Hole the fluxes to the ground (i.e., overland flows) which integrate rainfall, throughfall and litter leaching, are the main contributors to the stream flow. Deciphering the contribution of cycling through the vegetation from the atmospheric inputs in overland flows is then a crucial step for explaining the origin of stream fluxes. The single event sampling of throughfall prevents quantifying the canopy leaching. However, the throughfall compositions permit discriminating dry deposition (marine aerosols, dust) and canopy interaction. The slight Na increase from rainfall to throughfall, from 30 μmol L^{-1} (rainfall event of the throughfall sampling) to ~33 μmol L^{-1} ($n = 30$), is compatible with the 10% of canopy interception estimated by the COMFORT model for the Mule Hole SEW (Ruiz et al., 2010). These data suggest the non-addition or withdrawal of Na during interaction with the canopy. The fact that Na addition in throughfall was negligible explains why values calculated for dry deposition of other elements were so low (Table 2). For Na at least, rainfall collection with open bags integrates both the wet deposits and the soluble fraction of dry deposits, including marine aerosols. However, Cl enrichment observed in throughfalls, up to 10 times the rain value, cannot be ascribed to marine aerosols. Such enrichments are well documented for deciduous species in temperate climate and either attributed to HCl gaseous deposition, especially in areas impacted by acid rains, or to leaching of senescent leaves (e.g. Staelens et al. 2008).

Data in tropical forests are much scarcer but indicate that both sources may contribute. According to Franken et al. (1985) in Duke rainforest and to Cornu et al. (1998a) in the Amazonian forest, more than half of the Cl reaching the ground originates from canopy leaching. In contrast, in Cerrado, Lilienfein and Wickle (2004) attribute the Cl enrichment to dry deposition using Na as inert tracer. Using the same approach at Mule Hole, dry deposits are found negligible and cannot explain the Cl enrichment in throughfalls. The correlation of Cl concentrations with K ($R^2 = 0.72$, Fig. 4), itself a good proxy of canopy leaching (Cole and Rapp, 1980; Freiesleben et al., 1986; Lindberg et al., 1986; Braun et al., 2005), suggests that Cl enrichment may, partly, result from canopy leaching (Eichert and Fernandez, 2012). However, we cannot conclude whether a similar trend should be expected in case of significant HCl gaseous deposition. The relative contribution of HCl gaseous deposition and canopy leaching to throughfalls remains an open question.

At the ground surface, the Na flux to the ground (210 mol ha^{-1} yr^{-1}) was equivalent to the atmospheric input (242 mol ha^{-1} yr^{-1}, −13%), which is consistent with the absence of Na in the litter. The entire Na flux reaching the ground surface originated from atmospheric inputs: in the Mule Hole SEW, Na exhibited conservative behavior when rainwater passed through the canopy and interacted with litter at the ground surface. In contrast, the Cl flux reaching the ground surface (500 mol ha^{-1} yr^{-1}) was 68% higher than atmospheric inputs (296 mol ha^{-1} yr^{-1}): the Cl enrichment observed in throughfalls for a single event was also observed at the yearly scale in the fluxes reaching the ground surface. The average Cl/Na molar ratio in throughfall, 2.68, is close to that of overland flows, 2.37. This suggests that Cl addition occurred mainly at the canopy level and not during litter leaching, although leaching experiments performed on leaves of the main tree species of Mule Hole indicate that litter releases small amounts of labile Cl (Audry et al., 2014). Assessment of Cl sources to the ground will require more specific monitoring of dry deposits.

The evolution of chemical composition from rainfall to overland flow was also accompanied by strong enrichments in Si, Ca, Mg and K (Table 2). The K/Na molar ratio increased sharply from rainfall (0.4) to throughfall (7.4) but remained almost constant in overland flows (8.6) confirming that canopy leaching is the dominant source of K (85%) to the ground surface (e.g. Lovett and Lindberg, 1984; Grimaldi et al., 2004). Ca/Na and Mg/Na gradually increased from rainfall to throughfall, from 1.2 to 3.9 and from 0.3 to 1.5, respectively, and to the ground surface, 8.7 and 3.5 respectively; both canopy and litter leaching contribute to the Ca and Mg fluxes reaching the ground surface, with a probable higher contribution from litter, as observed by Cole and Rapp (1980) for temperate forests. Alkalinity follows an evolution similar to Ca and Mg, indicating that litter leaching and to a lesser extent canopy produce alkalinity. Si/Na ratio exhibited an opposite behavior to K/Na, with low values in rainfall and throughfall, 0.15 and 0.9 respectively, and high value, 14.7 at the ground surface. The slight increase of Si/Na ratio from rainfall to throughfall could have partly resulted from canopy and/or silicate dust leaching since *A. latifolia* throughfalls exhibited small but significant Si concentrations, 19 μmol L^{-1} on average, even though the leaves do not contain any measurable Si. If we assume that the Si concentration of *A. latifolia* throughfalls resulted entirely from dust leaching and that the Si/K molar ratio (19/447 = 0.043) of *A. latifolia* throughfalls is representative of dust contribution for all throughfalls, the dust leaching would then account for 60 mol ha^{-1} yr^{-1}, i.e., 3% of the Si flux to the ground surface, which is again close to values found in the humid forest of Amazonia (Cornu et al., 1998b).

Relative enrichments of Si from throughfall to overland flows indicate that the Si concentration in overland flows was controlled by ground surface processes. Occurrence of Na-plagioclase and quartz dissolution at the ground surface can be ruled out, as the dissolution rates of these two minerals are extremely low (White and Brantley, 1995), and as similar Na concentrations were found in overland flows and in rains. Similarly, the Si concentration in overland flow, on average 200 μmol L^{-1}, was well above the equilibrium silica concentration for kaolinite dissolution, 40 μmol L^{-1} (Nordstrom et al., 1990). The only pool compatible with fast and significant Si dissolution is the phytoliths released during litter decay, whose dissolution rate is almost two orders of magnitude higher than the dissolution rate of clay minerals at neutral pH (Köhler et al., 2003; Fraysse et al., 2010).

The observed Si concentrations of overland flow compared well with expected values using experimental dissolution rates of litter. Assuming that litter would be in permanent interaction with rain water, the theoretical silica concentration resulting from interaction with litter can be estimated from the relationship (adapted from Fraysse et al., 2010):

$$C_{Si} = D \cdot M/P \quad (27)$$

with D the experimental dissolution rate of Si (mol g^{-1} yr^{-1}), M the dry litter mass in the ecosystem (g_{dw} ha^{-1}) and P the annual precipitation (L ha^{-1} yr^{-1}). Applied to the Mule Hole SEW with an average 2009–2010 litter mass of 5.10^6 g_{DW} ha^{-1}, a mean annual rainfall of 1100 mm yr^{-1} (1.1×10^7 L ha^{-1} yr^{-1}) and a Si dissolution rate from litter at neutral pH of 10^{-6} mol g_{dw}^{-1} day^{-1}, the estimated Si concentration that could be attributed to litter leaching would be 166 μmol L^{-1}. This value is close to the average concentration of the Si measured in overland flows, which includes about 30 μmol L^{-1} from throughfall. However, overland flow monitoring suggests that litter leaching does not proceed at constant rate. The DOC concentration normalized to atmospheric inputs (DOC/Na) increased by a factor of 6 to 7 over the rainy season and culminated at the end of the monsoon in October–November (Fig. 6). As observed in other dry tropical deciduous forests (Sarjubala Devi and Yadava, 2007), litter decay rate increased throughout the rainy season when rainfall and soil moisture were the highest, explaining why litter decay is efficient in such forests (Sundarapandian and Swamy, 1999). The positive correlation between Si/Na and DOC/Na ratios in overland flows ($R^2 = 0.92$) suggests that the Si leaching rate from litter increases as the litter decay rate increases. Such behavior

differs from temperate and boreal forests where litter decay lasts for several years and carbon leaching precedes silica, leading to silica accumulation in the Oi horizon as litter ages (Ellenberg et al., 1986; Fraysse et al., 2010).

The dissolved silica flux to the ground surface was almost equivalent to the solid flux associated with the annual leaf and herbaceous litter fall (Table 3), indicating that litter leaching was complete for this element. Since silica concentration in overland flow (200 μmol L^{-1}) exceeded saturation with kaolinite and quartz ($K_{eq\ quartz} = 10^{-4}$, Langmuir, 1997), kaolinite and quartz should be preserved after infiltration of overland flow solutions in the Mule Hole soils. This confirms the role of vegetation turnover for controlling the soil minerals in dry tropical forests Lucas (2001).

Overland flows also exhibited seasonal trends between DOC/Na and Ca/Na, Mg/Na, Alkalinity/Na and partly K/Na (on Ferralsol–Vertisol transition but not on Ferralsol; Fig. 6 and Section 4.2) suggesting that litter leaching also controlled the alkalinity, DOC and partly the Ca and Mg solute fluxes reaching the ground, with increasing efficiency throughout the rainy season. Since canopy leaching contributed to the solute fluxes measured in overland flows, it was therefore not possible to separate the contribution of litter leaching and compare it to dry litter fall. However, as the contribution of vegetation cycling to the solute flux of Ca above the ground surface accounted for only one third of the Ca flux associated with dry litter, litter leaching should contribute minimal Ca. Two mechanisms can account for the poor recovery of Ca: (1) the variability of litter decay rates among leaf/herb litter species (e.g., Songwe et al., 1995; Wieder et al., 2009 for wet tropical forest), as Ca concentration in dry litter varies by one order of magnitude according to species (Table 3), or (2) direct recycling of Ca from litter to roots by microbial and/or fungal activity. This latter process was identified for P (Herrera et al., 1978), but direct absorption of apatite-derived Ca by mycorrhizae was also envisaged as a mechanism for supplying trees (Blum et al., 2002). Identifying which mechanism dominates would require experiments of litter leaching. The contrasting recoveries of Si and Ca in leachates from litter confirmed that litter decay in dry tropical forests is not a congruent process (e.g. Songwe et al., 1995; Rogers, 2002).

5.1.2. Origin of the solutes in soil output flux

The only dissolved element released from the soil profile was Na, with a net output flux ($F_{x\ soil}$) of 651 mol ha^{-1} yr^{-1}. As the exchangeable Na pool is negligible (~1 mmol kg^{-1}, Violette et al., 2010b), the net dissolved Na flux from the soil profile can be confidently assigned to on-going chemical weathering of Na-plagioclase. Then, according to the Eqs. (20) and (22), the Na flux produced by soil at the watershed scale was composed of 77% of plagioclase-derived Na and 23% of atmospheric inputs.

The other major solute species K, Ca, Mg, Cl and Si, whose fluxes to the ground were enhanced by vegetation cycling, were depleted compared to soil input fluxes ($\Delta F_{x\ soil} < 0$), which means that for these species the soil acted as a sink. The dissolved fluxes removed from the soil profile range from 36% for Cl to 92% for K. In the case of Cl, the flux removed from pore water ($\Delta F_{ci\ soil} = 164$ mol ha^{-1} yr^{-1}) was almost equivalent to the flux originating from canopy leaching (~200 mol ha^{-1} yr^{-1}, see previous section). As a consequence, the soil output flux of Cl equals the atmospheric input flux (Table 2), suggesting that pedogenic processes such as microbial exchange, soil particle exchange of Cl or chlorination of organic matter (Bastviken et al., 2006, 2007) were not significant or occurred at steady state. It can be deduced from Eqs. (21) and (22) that 59% of Cl of soil outputs were derived from open field deposits and 41% from canopy leaching and/or HCl gaseous deposition.

The fluxes of K, Ca and Mg retained in the average soil cover also coincided with those added by vegetation cycling above the ground (Table 2): at the scale of the soil–plant profile the behavior of these elements can be considered as internal cycling. However, discrepancies existed for Ca according to the soil type: output fluxes of Ca were four times higher in Vertisol than in Ferralsol. According to the WITCH model, the Ca and Mg fluxes in Vertisol could be involved in a succession of dissolution/precipitation of calcite, Ca- smectite and Mg-smectite (Violette et al., 2010a). Sorption processes may also be involved in the solute balance of K, Ca and Mg in soils. The cation exchange capacity (CEC) in the Ferralsol was monotonous with depth and composed of 11 cmol kg^{-1} for Ca (70% of the total CEC), 3.8 cmol kg^{-1} for Mg (25%) and 0.5 for K (3%), whereas in the Vertisol it evolves with depth from 9.6 to 21 cmol kg^{-1} for Ca (57% of the total CEC), from 4.6 to 15 cmol kg^{-1} for Mg (40%). The exchangeable fraction of K in the Vertisol was constant and lower than in Ferralsol, 0.35 cmol kg^{-1} (1%). The exchangeable stocks of K, Ca and Mg within the 2 m of soil layer were equivalent to about 100 years of dissolved K input to the soil and to 2000 to 5000 years of Ca and Mg inputs depending on the soil type. However, if sorption was controlling the solute budget of these three elements in soils, the CEC composition should have contained a higher proportion of K, as it is the most abundant cation in the input flux and as kaolinite has relatively strong affinity for K adsorption (Levy et al., 1988). The fact that K was 20–50 times less adsorbed than Ca in both soils indicated that K uptake by plant roots prevails over adsorption onto clays. In Ferralsols, the Mg/Ca ratio of pore water increased compared to the soil inputs: a larger proportion of Ca was removed from the soils, which is compatible with both vegetation uptake and adsorption onto clays (e.g. Udo, 1978). In Vertisols, the Mg/Ca ratio of pore waters decreased slightly, which is only possible if a net Mg-smectite precipitation was balancing the preferential plant root uptake and the Ca adsorption onto clays. Since $\Delta F_{X\ soil} < 0$ for these three elements, Eqs. (21) and (22) indicate that 78% of Ca, 90% of Mg and 93% of K in the soil outputs have transited through the vegetation and the remaining 22%, 10% and 7% respectively were derived from atmospheric inputs.

The silica behavior within the soil was intermediate between “plant-driven” and “weathering-driven” elements: the soil output represented more than one third the input flux. The net Na output flux from soils suggests that Na-plagioclase weathering contributed to the Si output flux.

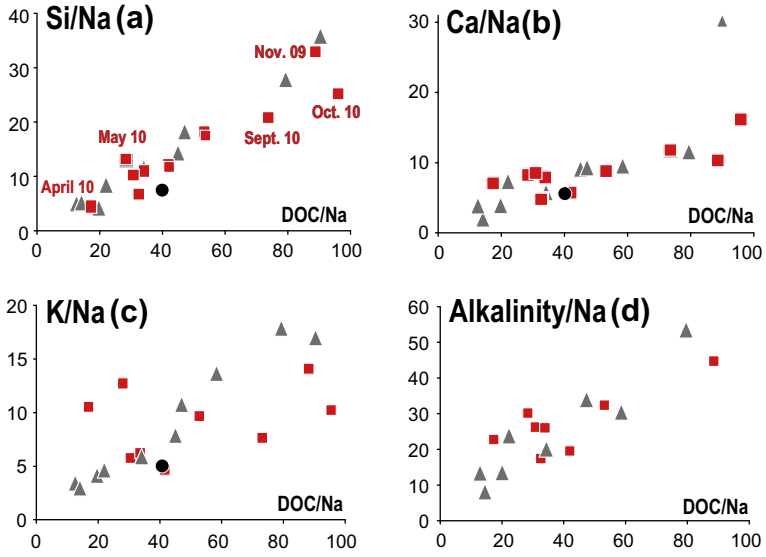

Fig. 6. Comparison between DOC/Na ratio and Si/Na (a), Ca/Na (b), K/Na (c) and Alkalinity/Na (d) ratios in overland flows: on Ferralsol red squares, on Ferralsol–Vertisol transition grey triangle, on Vertisol black dot. Trends observed are independent of the nature of soils over which they are flowing, except for the K/Na ratio over Ferralsol. They correspond to a temporal evolution of overland flow composition during the rainy season. (For interpretation of the references to colour in this figure legend, the reader is referred to the web version of this article.)

Since infiltrated solutions were oversaturated with kaolinite, Na-plagioclase likely breaks down into kaolinite, the most ubiquitous mineral in the Mule Hole Ferralsol. At equilibrium and using the average Na-plagioclase composition determined by Braun et al. (2009), the weathering reaction would be:

$$2(Na_{0.92}Ca_{0.08})(Al_{1.07}Si_{2.93})O_8 + 2H^+ + 9H_2O \rightarrow 1.07Si_2Al_2O_5(OH)_4 + 1.84Na^+ + 0.16Ca^{2+} + 3.72H_4SiO_4 \quad (28)$$

Using the net output flux of Na (651 mol ha^{-1} yr^{-1}) as a proxy of the fluxes released by the above reaction, the $F_{X\ weathering}$ for Ca and Si was 57 and 1302 mol ha^{-1} yr^{-1}, respectively. Taking into account this weathering flux, the amount of dissolved silica actually removed from soil solution was 2448 mol ha^{-1} yr^{-1} (1146 + 1302), i.e. about twice the amount initially deduced from the silica balance. Precipitation of amorphous silica within the soil can be discarded because silica concentrations in soil seepages, 600 μmol L^{-1}, were under the saturation limit of amorphous silica ($\sim 2 \times 10^3$ μmol L^{-1}, $\log K = -2.71$; Parkhurst and Appelo, 1999). Rather, the Si deficit might be attributed to root uptake. According to Eqs. (19)–(21) and taking into account the possible contribution of Na-plagioclase weathering, 1% of the soil output fluxes of Si originated from atmospheric inputs (dust leaching), 48% from vegetation cycling and 51% from current weathering. the proportion of Si from primary silicate weathering was very close to the value of 55% reported by Gérard et al. (2008) for a temperate forest, which they obtained by combining mass balance and reactive transport modeling. This balance illustrates the complexity of the silica cycling, as Si is involved in many biotic and abiotic processes. Taking into account Na-plagioclase weathering leads to the following estimation of the origin of soil output fluxes of Ca: 74% transited through the vegetation, 21% was derived from atmospheric inputs and 5% was derived from weathering.

5.2. Element origin in the stream

5.2.1. At the flood event scale: Mixing analysis

The EMMA has been validated by calculating squared coefficient of determination (R^2) between predicted and measured solute concentrations. For October 2008 storm events, R^2 ranges between 0.81 (Ca) and 0.98 (Mg), the EMMA model being a strong ($R^2 > 0.75$) predictor of all the solutes. The comparison of the predicted and observed mean indicates that EMMA smoothed the variations of Cl and Na concentrations, and failed to reproduce the higher concentrations observed during flow recession. This limitation may be attributed to the absence, in the inversion, of a "pure" seepage end-member. However, predicted Na and Cl mean weighted concentrations are close to the measured ones. Predicted Si, K, Ca and Mg mean concentrations also fit within 10% the observed values.

During rainfall events, stream flow was dominated by contributions from rainfall and throughfall end-members, up to 40% and 34% respectively, and down to 0% during recession periods (9a). The throughfall contribution tended to decrease with time from the first storms to the last ones at the end of the October. This can be explained by a more intense canopy leaching during the early rainy events, which is consistent with the decrease of the K/Na molar ratio in the stream throughout October (Fig. 7b).

Seepage inputs into stream water should constitute the complementary contribution, minimal during rain events and increasing during recession periods. However, the

quickflow is the only end-member able to properly explain the whole chemistry of the stream water. Its composition is a mixture of overland flow and seepage, i.e., two pools of water that are not supposed to contribute to the stream at the same time: overland flow should complement peak flows whereas seepages should dominate during recession periods. The dichotomy of these two pools is illustrated by the contrasting evolutions of the Si/Na and Na/Cl molar ratios at the flood event scale, considered as proxies of litter leachate (then overland flow) and Na-plagioclase weathering (then seepage), respectively (Fig. 7b): The Si/Na ratio increased during peak flows whereas the Na/Cl ratio increased during flood recessions. Thus, the relative contributions of seepage and overland flow cannot be distinguished from one another using the EMMA, which prevents a precise quantification of these end-members. However, the EMMA showed that the overland flow origin varied at the storm scale level and, accordingly, that the nature of the vegetation contribution (canopy interaction or litter leaching) fluctuated as well at this scale. Since vegetation contribution to the stream depends mainly on the relative overland flow or near-surface flow contributions, indirect comparison with other tropical watersheds is possible using storm flow deconvolution. For instance, in the humid context of the Guyana rainforest ($P = 3500$ mm yr^{-1}), the overland flow component still provides 24% of Si, 25% of Ca, 29% of Mg and 37% of K to the chemical flux exported by the stream during a storm event (Grimaldi et al., 2004) and, as in our work, K is assigned to throughfall and Ca and Mg to litter leaching. The origin of silica, about 10 times less concentrated than at Mule Hole, could not be precisely determined in the Guyana watershed. In the montane rainforest of Ecuador (similar context, $P = 2000$ mm yr^{-1}), Boy et al. (2008) estimate that storm flow and lateral flow account for one third of K, Ca, Mg and Na export. These proportions include an almost constant baseflow fraction, explaining why Na, not found in the O horizon, contributes to the export of solutes. These examples suggest that transit through the vegetation contributes significantly to solute fluxes exported from tropical forested watersheds when overland flow is involved in the stream flow.

5.2.2. At the seasonal/yearly scale

The evolution of the stream composition during the rainy seasons 2005 and 2009 (Fig. 8) was consistent with

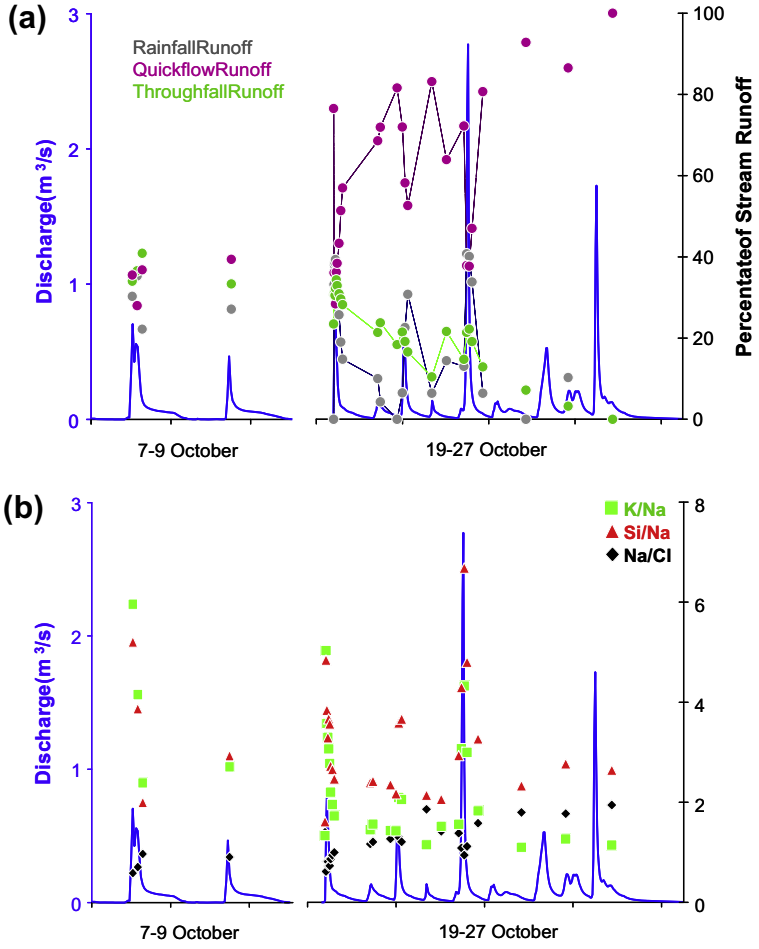

Fig. 7. (a) EMMA calculated contributions of rainfall, throughfall and quickflow to the stream floods of October 2008; (b) evolution of the Mule Hole stream chemistry (Na/Cl, K/Na and Si/Na) for the same period.

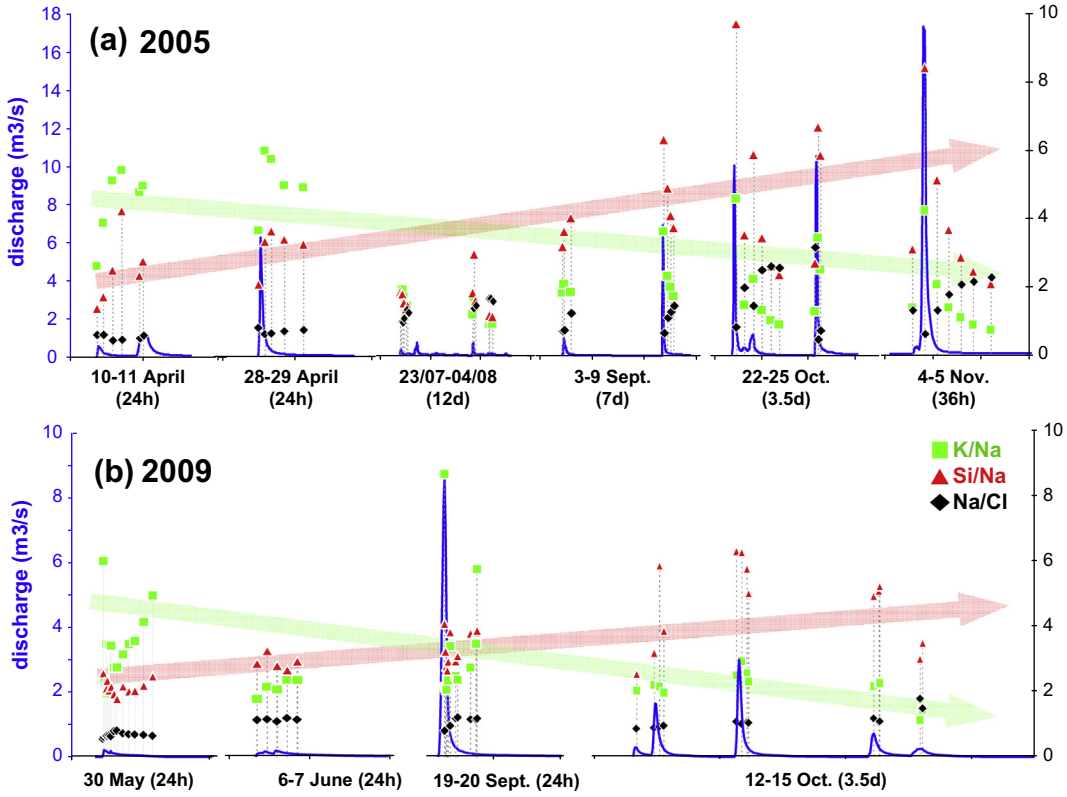

Fig. 8. Typical variations of Na/Cl, K/Na and Si/Na within stream storms and along a rainy season at Mule Hole for the years 2005 (a) and 2009 (b). The Na/Cl molar ratio, which may be considered as a relative proxy for primary silicate (albite) weathering, decreases during peak flow. The K/Na and Si/Na ratios increase during peak flows, indicating that K and Si, but also Ca, Mg and alkalinity (not shown) are not related to Na fluxes. Over the year, the K/Na ratio tends to decrease whereas the Si/Na ratio increases and the Na/Cl ratio remains constant.

Table 4
Percentage of solutes originating from transit through the vegetation, current weathering and atmosphere in overland flows and soil outputs (seepages).

Element sources	DOC	Alkalinity	Si	Cl	Na	K	Ca	Mg
In overland flows								
Atmospheric inputs (%)	15	5	3	51	100	8	16	11
Vegetation cycling (%)	85	95	97	49	0	92	84	89
In Ferralsol seepage								
Atmospheric inputs (%)	15	5	1	49	18	8	15	16
Vegetation cycling (%)	85	95	48	51	0	92	79	84
Direct chemical weathering (%)	0	0	51	0	82	0	6	0

observation at short times scales. For instance, the progressive decrease of K/Na molar ratios with successive storms of October 2008 account partly for the seasonal decrease observed in 2005 and 2009. It may reflect the decrease of canopy leaching during the rainy season as observed in other tropical forests (e.g. Chuyong et al., 2004) or the possible dilution of canopy leaching by heavier rains. The gradual increase of the Si/Na ratio in the stream throughout the rainy season also followed the seasonal evolution of overland flows (Fig. 6a), showing from a qualitative point of view the direct impact of litter decay on the stream composition. The seepage contribution, identifiable from Na/Cl values >1 (Fig. 8), was absent in the first storms, as the soil layer was still not saturated by water (Descloitres et al., 2008), but later contributed to the recession of major storms once the soil layer was water-saturated.

The annual contributions of atmospheric inputs, transit through the vegetation and "direct" weathering to the stream fluxes can be retrieved in two steps. First, the consistency between measured annual chemical fluxes in the stream and those derived from theoretical mixtures of overland flow and seepage, as estimated by the hydrological model (Section 4.1), was checked. Then, the contributions of atmospheric inputs, transit through the vegetation and

"direct" weathering estimated separately for the overland flow and the seepage (section 5.1 and Table 4) were propagated at the stream level. Apart from an overestimation of the Na concentration by 50% (Table 5), the predicted fluxes fit the measured ones (difference < 20%), which confirms that the model provided a realistic estimate of the water contributions at the stream outlet. The overestimation of the computed Na flux can be explained by a slight overestimation of the seepage contribution, since the Na concentration in Ferralsol seepage was about 25 times the Na concentration in overland flow. A seepage contribution of 6 mm instead of the 12 mm computed by the hydrological model would be required for explaining the low Na concentrations of the stream.

Estimated proportions of atmospheric inputs, cycling through the vegetation and chemical weathering contributing to the stream (Table 5) confirmed that most of the dissolved Si, K, Ca, Mg, alkalinity and possibly half of the Cl (on the condition that gaseous deposits would be negligible) of the stream would have transited through the vegetation while "direct" chemical weathering contributed only a small fraction of Na and silica fluxes. Taken as a whole, as much as 80–90% of the total dissolved load in the stream would have transited through the vegetation. This large proportion was probably partly due to the specific context of the Mule Hole SEW, including the vegetation cover (forest) and the climatic conditions (sub-humid tropical). Indeed, intense evapotranspiration by the forest prevents base-flow contribution and favors overland flow and the subsequent flush of litter decay components (Berner et al., 2003; Zakharova et al., 2007), whereas tropical conditions induce rapid litter decay and enhance nutrient mobility. In the literature, the few works where contribution of vegetation cycling to stream composition is assessed also find high values in the tropical environment. Based on Ge–Si signatures of Hawaiian rivers, Derry et al. (2005) estimate that phytolith dissolution accounts for 68–90% of the dissolved Si exported by these tropical rivers, which is very close to values found for the Mule Hole SEW. The intensity of silica cycling by tropical forests would then be as important as it is for Ca, Mg and K nutrients, and may regulate the silica flux exported by tropical rivers, which account for 74% of the riverine Si input to ocean (Martin et Meybeck, 1979). Surprisingly, in boreal environments, which are cold climates with significant base flow sustaining rivers, plant-litter degradation still accounts for 10–40% of the solute fluxes exported (Zakharova et al., 2007).

To summarize, the approach combining solute mass balances at both soil–plant profile and stream scales, themselves based on high density geochemical measurements and accurate hydrological balance, improved the current knowledge about the origin of the solute fluxes exported out of the watershed, and particularly the role of vegetation. One important finding was the discrepancy between the averaged seasonal composition of canopy + litter leachates and the biomass composition. For instance, throughfall contribution enhanced the K flux while only a small proportion of Ca was recovered from litter leachates of Mule Hole. Therefore, overland flow composition (Ca/K = 0.99) provided a better estimation of vegetation contribution to the stream (Ca/K = 0.97) than the litter composition (Ca/K = 3.05 to 3.93). Moreover, it is confirmed that weathering processes within the soil layer are likely influenced by vegetation. On one hand, infiltrating solutions are enriched in nutrients, alkalinity and silica that may reduce the aggressiveness of solutions interacting with clay minerals of soils and contribute to their stability (e.g. Lucas, 2001). On the other hand, the K, Ca, Mg and Si fluxes leaving the soil horizon may partly or totally originate from infiltration and then not reflect weathering of bedrock and/or secondary minerals. Accordingly, the stream base flow may not represent the "pure" chemical

Table 5
Comparison between observed solute annual fluxes and those predicted using the hydrological model and concentrations of overland flows and soil seepages, and percentage of each solute source (transit through vegetation, current weathering and atmosphere) in the stream.

	Discharge	DOC	Alkalinity	Si	Cl	Na	K	Ca	Mg
	mm	mol/ha							
2005	179	752	686	288	74	63	156	168	117
2006	45	325	276	121	31	43	51	75	43
2008	23	140	89	35	10	9	27	28	16
2009	50	289	312	77	20	20	77	65	30
4 yr average	74	376	341	130	34	34	78	84	51
2005–2006 average	112	538	481	204	53	53	103	121	80
Modeling* 2004–2006	94	578	394	214	60	82	112	116	71
Difference between model and 2005–6 average (%)	−16	7	−18	5	15	55	8	−4	−11
Element sources (4 yr average)									
Atmospheric input (mol/ha)		56	17	4	17	30	6	13	6
(%)		15	5	3	50	90	8	16	12
Transit through vegetation (mol/ha)		320	324	117	17**	0	72	70	45
(%)		85	95	90	50**	0	92	83	88
Current chemical weathering (mol/ha)				9	0	3	0	1	0
(%)				7	0	10	0	1	0

* Origin of fluxes from hydrological model: 12 mm/yr seepage, 53 mm/yr OF red soil, 29 mm/yr OF black soil (Violette et al., 2010a).
** Includes an unknown fraction of gaseous deposits.

weathering end-member, leading to a slight overestimation of mineral weathering rates calculated from base flow composition. Finally, solute mass balance within the soil provided only a first order estimation of chemical weathering *vs* plant uptake: Aggrading or degrading biomass may impact both solute mass balance and mineral weathering in unknown extent. This could be quantified using for instance the isotopic fractionations of the elements involved (Si, Ca, Mg...) or combined models. If existing physical, chemical and biological models do not "adequately quantify the inter-relationship and coupling between all of the important processes" (Brantley et al., 2012b), models can, however, constitute powerful tools for assessing the respective effects of infiltrating water chemistry, evapotranspiration, chemical weathering and vegetation uptake on solute mass balances. We demonstrated that in the stream, silica and alkalinity fluxes are also dominated by transit through the vegetation. None of these species were linked to "current weathering". Na was the best proxy of primary silicate weathering, which is consistent with observations of Braun et al. (2009) and Price et al. (2012, 2013).

6. CONCLUSION

The forested SEW of Mule Hole is characterized by a high evapotranspiration that leads to disconnection between stream and deep groundwater flows, resulting in control of the stream flow by surface processes. In this context, the impacts of vegetation element cycling on solute fluxes exported at the scale of 1D soil–plant profile and then at the stream level were studied. The main conclusions are:

- At the scale of a 1D soil–plant profile, vegetation cycling contributes significantly to the ground surface fluxes of Si, K, Ca, Mg and possibly of Cl (on the condition that gaseous deposits of Cl would be negligible, which couldn't be assessed). Flux of K was mostly associated with canopy leaching, Si with litter leaching and Ca and Mg evenly distributed between canopy and litter leaching. Litter leaching is not a congruent process: while Si and Mg associated to the dry litter flux were almost entirely recovered in litter leaching, only a small fraction of Ca and K was. The composition of canopy + litter leachates evolved throughout the rainy season, with a maximum of litter leaching in October–November. Assessing the vegetation contribution to solute fluxes in a stream therefore requires monitoring of solutions reaching the ground.
- The soil output fluxes of K, Ca, Mg, Si and Cl were depleted compared to the inputs and can be considered as relicts of infiltration, which suggested that vegetation contribution still predominated in soil outputs. This means that in rivers sustained by base flow, base flow composition might not reflect solely the water–rock interactions.
- The solute fluxes of K, Ca, Mg and Si attributed to vegetation cycling represented 15 to 20 times the solute fluxes exported by the stream. The proportion of elements that transited through the vegetation ranged from 83 to 97% for Si, K, Ca, Mg and alkalinity. Accordingly, active chemical weathering accounted for a maximum of 10% of Na and silica and less than 3% of K, Ca and Mg. Overall, 80 to 90% of the total dissolved solids (TDS) exported by the stream have transited through the vegetation.

Our study demonstrates that under this tropical, subhumid climate, vegetation was controlling the solute fluxes exported by the stream. This process could not have been predicted only from chemical mass balances at the outlet. Effect of vegetation can be described as a dual function; one, indirect, is evapotranspiration that limits the runoff and decreases aggressiveness of pore waters towards soil minerals. The other, direct, consists of enhancing solute fluxes through a vertical cycling that brings leachable nutrients –including silica and alkalinity- to the ground surface and then to the outlet. Since direct and indirect effects evolve throughout the year, estimating the impact of vegetation on solute flux requires an extensive monitoring and accurate knowledge of the hydrological functioning of the watershed. Our approach provides a good basis for calibrating geochemical models and more precisely assessing the role of vegetation on soil processes.

ACKNOWLEDGMENTS

The Mule Hole basin is part of the ORE-BVET project (Observatoire de Recherche en Environnement – Bassin Versant Expérimentaux Tropicaux, http://bvet.omp.obs-mip.fr/index.php/eng/) supported by the French Institute of Research for Development (IRD), CNRS and Toulouse University. The project also benefited from funding from INSU/ CNRS (Institut National des Sciences de l'Univers/Centre National de la Recherche Scientifique) through the French program EC2CO (Ecosphère Continentale et Côtière) and from the ACI-Eau. The authors are thankful to the four anonymous reviewers and to the Associate Editor whose comments considerably improved the quality of the manuscript. We thank the Karnataka Forest Department and the staff of the Bandipur National Park for all the facilities and support they provided.

REFERENCES

Amundson R., Richter D. D., Humphreys G. S., Jobbágy E. G. and Gaillardet J. (2007) Coupling between Biota and earth materials in the critical zone. *Elements* **3**, 327–332.

Audry S., Akerman A., Riotte J., Oliva P., Maréchal J. C., Fraysse F., Pokrovsky O. and Braun J. J. (2014) Contribution of forest fire ash and plant litter decay on stream dissolved composition in a sub-humid tropical watershed (Mule Hole, Southern India). *Chem. Geol.* **372**, 144–161.

Barbiero L., Parate H. R., Descloitres M., Bost A., Furian S., Mohan Kumar M. S., Kumar C. and Braun J. J. (2007) Using a structural approach to identify relationships between soil and erosion in a semi-humid forested area, South India. *Catena* **70**, 313–329.

Bastviken D., Sanden P., Svensson T., Stahlberg C., Magounakis M. and Oberg G. (2006) Chloride Retention and Release in a Boreal Forest Soil: Effects of Soil Water Residence Time and Nitrogen and Chloride Loads. *Environ. Sci. Technol.* **40**, 2977–2982.

Bastviken D., Thomsen F., Svensson T., Karlsson S., Sanden P., Shaw G., Matucha M. and Oberg G. (2007) Chloride retention in forest soil by microbial uptake and by natural chlorination of organic matter. *Geochim. Cosmochim. Acta* **71**, 3182–3192.

Berner E.K., Berner R.A., Moulton K.L. (2003) Plants and mineral weathering: present and past. In: Drever J.I. (ed.), Treatise on Geochemistry, Vol. 5. Surface and Groundwater, Weathering, and Soils. Elsevier. pp. 169–188.

Blum J. D., Klaue A., Nezat C. A., Driscoll C. T., Johnson C. F., Siccama T. G., Eagar C., Fahey T. J. and Likens G. E. (2002) Mycorrhizal weathering of apatite as an important calcium source in base-poor forest ecosystems. *Nature* **417**, 729–731.

Brantley S. L., Lebedeva M. and Hausrath E. M. (2012a) A geobiological view of weathering and erosion. In *Fundamentals of Geobiology* (eds. A. H. Knoll, D. E. Canfield and K. O. Konhauser). Blackwell Publishing, pp. 205–225.

Brantley S. L., Lebedeva M. and Hausrath E. M. (2012) A geobiological view of weathering and erosion. In *Fundamentals of Geobiology* (eds. A. H. Knoll, D. E. Canfield and K. O. Konhauser. pp. 205–227.

Bormann B. T., Wang D. F., Bormann F. H., Benoit G., April R. and Snyder M. C. (1998) Rapid, plant-induced weathering in an aggrading experimental ecosystem. *Biogeochemistry* **43**, 129–155.

Bowser C. J. and Jones B. F. (2002) Mineralogic controls on the composition of natural waters dominated by silicate hydrolysis. *Am. J. Sci.* **32**, 582–662.

Boy J., Valarezo C. and Wickle W. (2008) Water flow paths in soil control element exports in an Andean tropical montane forest. *Eur. J. Soil Sci.* **59**, 1209–1227.

Braun J.-J., Ndam Ngoupayou J. R., Viers J., Dupre B., Bedimo Bedimo J. P., Boeglin J. L., Robain H., Nyeck B., Freydier R., Sigha Nkamdjou L., Rouiller J. and Muller J.-P. (2005) Present weathering rates in a humid tropical watershed: Nsimi site (South Cameroon). *Geochim. Cosmochim. Acta* **69**, 357–387.

Braun J. J., Descloitres M., Riotte J., Fleury S., Barbiero L., Boeglin J. L., Violette A., Lacarce E., Ruiz L., Sekhar M., Mohan Kumar M. S., Subramanian S. and Dupré B. (2009) Regolith mass balance inferred from combined mineralogical, geochemical and geophysical studies: Mule Hole gneissic watershed, South India. *Geochim. Cosmochim. Acta* **73**, 935–961.

Braun J.-J., Maréchal J.-C., Riotte J., Bœglin J.-L., Bedimo Bedimo J.-P., Ndam Ngoupayou J. R., Nyeck B., Robain H., Sekahr M., Audry S. and Viers J. (2012) Elemental weathering fluxes and saprolite production rate in a Central African lateritic terrain (Nsimi, South Cameroon). *Geochim. Cosmochim. Acta* **99**, 243–270.

Burns D. A., McDonnell J. J., Hooper R. P., Peters N. E., Freer J. E., Kendall C. and Beven K. (2001) Quantifying contributions to storm runoff through end-member mixing analysis and hydrologic measurements at the Panola Mountain Research Watershed (Georgia, USA). *Hydrol. Process.* **15**, 1903–1924.

Campo J., Manuel Maass J., Jaramillo V. J. and Martinez Yrizar A. (2000) Calcium, potassium and magnesium cycling in a Mexican tropical dry forest ecosystem. *Biogeochemistry* **49**, 21–36.

Chadwick O. A. and Chorover J. (2001) The chemistry of pedogenic thresholds. *Geoderma* **100**, 321–353.

Christophersen N. and Hooper R. P. (1992) Multivariate-analysis of stream water chemical data—the use of principal component analysis for the end-member mixing problem. *Water Resour. Res.* **28**, 99–107.

Chuyong G. B., Newbery D. M. and Songwe N. C. (2004) Rainfall input, throughfall and stemflow of nutrients in a central African rain forest dominated by ectomycorrhizal trees. *Biogeochemistry* **67**, 73–91.

Cole D. W. and Rapp M. (1980) Elemental cycling in forest ecosystems. In *Dynamic Properties of Forest Ecosystems* (ed. D. E. Reichle). International Biological Programme 23. Cambridge University Press.

Cornu S., Ambrose J. P., Lucas Y. and Desjardins T. (1998a) Origin and behaviour of dissolved chlorine and sodium in Brazilian rainforest. *Water Res.* **32**, 1151–1161.

Cornu S., Lucas Y., Ambrosi J. P. and Desjardins T. (1998b) Transfer of dissolved Al, Fe and Si in two amazonian forest environments in Brazil. *Eur. J. Soil Sci.* **49**, 377–384.

Derry L. A., Kurtz A. C., Ziegler K. and Chadwick O. A. (2005) Biological control of terrestrial silica cycling and export fluxes to watersheds. *Nature* **433**, 728–731.

Descloitres M., Ruiz L., Sekhar M., Legchenko A., Braun J. J., MohanKumar M. S. and Subramanian S. (2008) Characterization of seasonal local recharge using electrical resistivity tomography and magnetic resonance sounding. *Hydrol. Process.* **22**, 384–394.

Drever J. I. (1994) Effects of plants on chemical weathering rates. *Geochim. Cosmochim. Acta* **58**, 2325–2332.

Eichert T. and Fernandez V. (2012) Uptake and release of elements by leaves and other aerial plant parts. In *Mineral Nutrition of Higher Plants* (ed. P. Marschner), 3rd edition, Academic Press. pp. 71–84.

Elliott S., Baker P. J. and Borchert R. (2006) Leaf flushing during the dry season: the paradox of Asian monsoon forests. *Global Ecol. Biogeogr.*, DOI: 10.1111/j.1466-822x.2006.00213.x.

Ellenberg H., Mayer R. and Schauermann J. (1986) *Ökosystemforschung– Ergebnisse des Sollingprojekts 1966–1986*. Verlag Eugen Ulmer, Stuttgart.

Fonseca W., Benayas J. M. R. and Alice F. E. (2011) Carbon accumulation in the biomass and soil of different aged secondary forests in the humid tropics of Costa Rica. *Forest Ecol. Manage.* **262**, 1400–1408.

Franken W., Leopoldo P. R. and Bergamin H. (1985) Nutrient flow through natural waters in "Terra Firme" forest in Central Amazon. *Turrialba* **35**, 383–393.

Fraysse F., Pokrovsky O. S. and Meunier J. D. (2010) Experimental study of terrestrial plant litter interaction with aqueous solutions. *Geochim. Cosmochim. Acta* **74**, 70–84.

Freiesleben N. E. V., Ridder C. and Rasmussen L. (1986) Patterns of acid precipitation to a Danish spruce forest. *Water Air Soil Pollut.* **30**, 135–141.

Gadd G. M. (2007) Biogeochemical transformations of rocks, minerals, metals and radionuclides by fungi, bioweathering and bioremediation. *Mycol. Res.* **III**, 3–49.

Gérard F., Mayer K. U., Hodson M. J. and Ranger J. (2008) Modelling the biogeochemical cycle of silicon in soils: application to a temperate forest ecosystem. *Geochim. Cosmochim. Acta* **72**, 741–758.

Grimaldi C., Grimaldi M., Millet A., Bariac T. and Boulègue J. (2004) Behaviour of chemical solutes during a storm in a rainforested headwater catchment. *Hydrol. Process.* **18**, 93–106.

Herrera R., Merida T., Stark N. and Jordan C. F. (1978) Direct phosphorus transfer from leaf litter to roots. *Naturwissenschaften* **65**, 208–209.

IUSS-Working-Group-WRB (2006) *World reference base for soil resources 2006*. World Soil Resources Food and Agriculture Organization of The United Nations, Rome.

Jaramillo V. J., Martínez-Yrízar A. and Sanford, Jr., R. L. (2011) Primary productivity and biogeochemistry of seasonally dry tropical forests. In *Seasonally Dry Tropical Forests: Ecology and Conservation* (eds. R. Dirzo et al). Island Press, pp. 109–128.

Kulshrestha U. C., Granat L., Engardt M. and Rodhe H. (2005) Review of precipitation monitoring studies in India – a search for regional patterns. *Atmos. Environ.* **39**, 7403–7419.

Langmuir D. (1997) Aqueous environmental Geochemistry. Prentice-Hall, 600p.

Legchenko A., Descloitres M., Bost A., Ruiz L., Reddy M., Girard J. F., Sekhar M., Mohan Kumar M. S. and Braun J. J. (2006) Resolution of MRS applied to the characterization of hard-rock aquifers. *Ground Water* **44**(4), 547–554.

Levy G. J., van der Watt H., Shainberg I. and du Plessis H. M. (1988) Potassium–calcium and sodium–calcium exchange on kaolinite and kaolinitic soils. *Soil Sci. Soc. Am. J.* **52**, 1259–1264.

Lilienfein J. and Wilcke W. (2004) Water and element input into native, agri- and silvicultural ecosystems of the Brazilian savanna. *Biogeochemistry* **67**, 183–212.

Lindberg S. E., Lovett G. M., Richter D. D. and Johnson D. W. (1986) Atmospheric deposition and canopy interactions of major ions in a forest. *Science* **231**, 141–145.

Liu F. J., Williams M. W. and Caine N. (2004) Source waters and flow paths in an alpine catchment, colorado front range, United States. *Water Resour. Res.* **40**, W09401. http://dx.doi.org/10.1029/2004WR003076.

Long S. P., Garcia Moya E., Imbamba S. K., Kamnalrut A., Piedade M. T. F., Scurlock J. M. O., Shen Y. K. and Hall D. O. (1989) Primary productivity of natural grass ecosystems of the tropics: a reappraisal. *Plant Soil* **115**, 155–166.

Lovett G. M. and Lindberg S. E. (1984) Dry deposition and canopy exchange in a mixed oak forest as determined by analysis of throughfall. *J. Appl. Ecol.* **21**, 1013–1027.

Lucas Y. (2001) The role of plants in controlling rates and products of weathering: importance of biological pumping. *Annu. Rev. Earth Planet. Sci.* **29**, 135–163.

Maréchal J. C., Murari R. R. V., Riotte J., Vouillamoz J. M., Mohan Kumar M. S., Ruiz L., Muddu S. and Braun J. J. (2009) Indirect and direct recharges in a tropical forested watershed: Mule Hole, India. *J. Hydrol.* **364**, 272–284.

Maréchal J. C., Braun J. J., Riotte J., Bedimo Bedimo J. P. and Boeglin J. L. (2011) Hydrological processes of a rainforest headwater swamp from natural chemical tracing in Nsimi Watershed, Cameroon. *Hydrol. Process.* **25**, 2246–2260.

Martin et Meybeck (1979) Elemental mass-balance of material carried by major world rivers. *Mar. Chem.* **7**, 173–206.

McDowell W. H. and Asbury C. E. (1994) Export of Carbon, Nitrogen, and major ions from three tropical montane watersheds. *Limnol. Oceanogr.* **39**, 111–125.

Moulton K. L., West J. and Berner R. A. (2000) Solute flux and mineral mass balance approaches to the quantification of plant effects on silicate weathering. *Am. J. Sci.* **300**, 539–570.

Nordstrom D.K., Plummer L.N., Langmuir D., Busenberg E., May H.M., Jones B., Parkhurst D.L. (1990) Revised chemical equilibrium data for major water-mineral reactions and their limitations. In: Melchior, D.C., Bassett, R.L. (eds) Chemical modeling of aqueous systems II. American Chemical Society, 398–413.

Paces T. (1983) Rate constraints of dissolution derived from the measurements of mass balance in hydrological catchments. *Geochim. Cosmochim. Acta* **47**, 1855–1863.

Parate H. R., Mohan Kumar M. S., Descloitres M., Barbiero L., Ruiz L., Braun J. J., Sekhar M. and Kumar C. (2011) Comparison of electrical resistivity by geophysical method and neutron probe logging for soil moisture monitoring in a forested watershed. *Curr. Sci.* **100**, 1405–1412.

Parkhurst D. L. and Appelo C. A. J. (1999) User's guide to PHREEQC (Version 2)-A computer program for speciation, batch-reaction, one-dimensional transport, and inverse geochemical calculations. US Geological Survey Water-Resources Investigations Report.

Prakasa Rao P. S., Momin G. A., Safai P. D., Pillai A. G. and Khemani L. T. (1995) Rain water and throughfall chemistry in the Silent Valley Forest in South India. *Atmos. Environ.* **29**, 2025–2029.

Price J. R., Hardy C. R., Tefend K. S. and Szymanski D. W. (2012) Solute geochemical mass-balances and mineral weathering rates in smallwatersheds II: Biomass nutrient uptake, more equations in more unknowns, and land use/land cover effects. *Appl. Geochem.* **27**, 1247–1265.

Price J. R., Rice K. and Szymanski D. (2013) Mass-balance modeling of mineral weathering rates and CO_2 consumption in the forested Hauver Branch watershed, Catoctin Mountain, Maryland, USA. *Earth Surf. Process. Landforms* **38**, 859–875.

Rice K. C. and Price J. R. (2014) Comparison of mass balances in two small forested watersheds on the upper and lower units of the Weverton Quartzite, Catoctin Mountain, Maryland, USA. *Aqu. Geochem.* **20**, 225–242.

Rogers H. M. (2002) Litterfall, decomposition and nutrient release in a lowland tropical rain forest, Morobe Province, Papua New Guinea. *J. Trop. Ecol.* **18**, 449–456.

Ruiz L., Varma M. R. R., Mohan Kumar M. S., Sekhar M., Maréchal J. C., Descloitres M., Riotte J. and Braun J. J. (2010) Water balance modelling in a tropical watershed under deciduous forest (Mule Hole, India): regolith matric storage buffers the groundwater recharge process. *J. Hydrol.* **380**, 460–472.

Sarjubala Devi A. and Yadava P. S. (2007) Wood and leaf litter decomposition of *Dipterocarpus tuberculatus* Roxb. in a tropical deciduous forest of Manipur, Northeast India. *Curr. Sci.* **93**, 243–246.

Singh L. and Singh J. S. (1991) Species structure, dry matter dynamics and carbon flux in a dry tropical forest in India. *Ann. Bot.* **68**, 263–273.

Siva Soumya B., Sekhar M., Riotte J. and Braun J. J. (2009) Non-linear regression model for spatial variation in precipitation chemistry for South India. *Atmos. Env.* **43**, 1147–1152.

Siva Soumya B., Sekhar M., Riotte J., Audry S., Lagane C. and Braun J. J. (2011) Inverse models to analyze the spatiotemporal variations of chemical weathering fluxes in a granito-gneissic watershed: Mule Hole, South India. *Geoderma* **165**, 12–24.

Songwe N. C., Okali D. U. U. and Fasehun F. E. (1995) Litter decomposition and nutrient release in a tropical rainforest, Southern Bakundu Forest Reserve. *Cameroon. J. Trop. Ecol.* **11**, 333–350.

Staelens J., Houle D., De Schrijver A., Neirynck J. and Verheyen K. (2008) Calculating dry deposition and canopy exchange with the canopy budget model: review of assumptions and application to two deciduous forests. *Water Air Soil Pollut.* **191**, 149–169.

Sundarapandian S. M. and Swamy P. S. (1999) Litter production and leaf-litter decomposition of selected tree species in tropical forests at Kodayar in the Western Ghats, India. *Forest Ecol. Manage.* **123**, 231–244.

Suresh H.S., Dattaraja H. S. Nandal N. and Sukumar R. (2011) Seasonally dry tropical forests in Southern Indian, an analysis of floristic composition, structure and dynamics in Mudumalai Wildlife Sanctuary. In *The ecology and conservation of seasonally dry forests in Asia* (eds. W. J. McShea, S. J. Davies and N. Bhumpakphan). Smithsonian Institution Scholarly Press. pp. 37–58.

Udo E. J. (1978) Thermodynamics of potassium-calcium and magnesium-calcium exchange reactions on a kaolinite soil clay. *Soil Sci. Soc. Am. J.* **42**, 556–560.

Velbel M. A. and Price J. R. (2007) Solute geochemical mass-balances and mineral weathering rates in small watersheds: methodology, recent advances, and future directions. *Appl. Geochem.* **22**, 1682–1700.

Violette A., Goddéris G., Maréchal J. M., Riotte J., Oliva P., Mohan Kumar M. S., Sekhar M. and Braun J. J. (2010a) Modeling the chemical weathering fluxes at the watershed scale in the Tropics (Mule Hole, South India): Relative contribution of the smectite/kaolinite assemblage versus primary minerals. *Chem. Geol.* **277**, 42–60.

Violette A., Riotte J., Braun J. J., Oliva P., Maréchal J. C., Sekhar M., Jeandel C., Subramanian S., Barbiero L. and Dupré B. (2010b) Formation and preservation of pedogenic carbonates in South India, links with paleomonsoon and pedological conditions: Clues from Sr isotopes, U–Th series and REEs. *Geochim. Cosmochim. Acta* **74**, 7059–7085.

Wieder W. R., Cleveland C. C. and Townsend A. R. (2009) Controls over leaf litter decomposition in wet tropical forests. *Ecology* **90**, 3333–3341.

White A. F. and Blum A. E. (1995) Effects of climate on chemical weathering in watersheds. *Geochim. Cosmochim. Acta* **59**, 1729–1747.

White A. F. and Brantley S. L. (Eds.) (1995) Chemical Weathering Rates of Silicate Minerals. Reviews in Mineralogy, vol. 31. Mineralogical Society of America, Washington, D.C. p. 584.

Zakharova E. A., Pokrovsky O. S., Dupré B., Gaillardet J. and Efimova L. E. (2007) Chemical weathering of silicate rocks in Karelia region and Kola peninsula, NW Russia: assessing the effect of rock composition, wetlands and vegetation. *Chem. Geol.* **242**, 255–277.

Zhang L., Dawes W. R. and Walker G. R. (2001) Response of mean annual evapotranspiration to vegetation changes at catchment scale. *Water Resour. Res.* **37**, 701–708.

Associate editor: Brian W. Stewart